Geomorphology 469 (2025) 109522

Contents lists available at ScienceDirect

Geomorphology

journal homepage: www.journals.elsevier.com/geomorphology

Assessing landslide susceptibility and dynamics at cultural heritage sites by integrating machine learning techniques and persistent scatterer interferometry

José Eduardo Bonini [a], Carlotta Parenti [b,c,*], Francesca Grassi [c,d], Francesco Mancini [c,d], Bianca Carvalho Vieira [a], Mauro Soldati [b,c]

[a] Geography Department, University of São Paulo, São Paulo, Brazil
[b] Department of Chemical and Geological Sciences, University of Modena and Reggio Emilia, Modena, Italy
[c] CRICT - Inter-Departmental Research and Innovation Centre on Constructions and Environmental Sciences, University of Modena and Reggio Emilia, Modena, Italy
[d] Department of Engineering "Enzo Ferrari", University of Modena and Reggio Emilia, Modena, Italy

ARTICLE INFO

Keywords:
Landslides
Cultural heritage
Random Forest
MT-DInSAR
Northern Apennines
Italy

ABSTRACT

Landslides can significantly affect cultural heritage sites worldwide, often leading to irreversible damage and loss of invaluable cultural assets, and the assessment of the spatio-temporal distribution of such processes in culturally relevant sites is still a challenge. In this study, we propose a workflow to assess landslide susceptibility at the catchment scale and landslide dynamics, in terms of state of activity, at the slope scale with reference to built environments. A fully open-source and quantitative approach that integrates machine learning methods and persistent scatterer interferometry is proposed. The workflow was tested to identify cultural heritage sites potentially affected by landslides in a catchment of the Northern Apennines (Italy) characterized by the occurrence of earth slides and earth flows. The research reveals that 18 sites are located in highly susceptible terrains and five of them display notable displacement rates. Two sites in the highest susceptibility class and with high displacements rates were selected as case studies. One of the sites showed displacement rates up to 8 mm/year, while the second one up to 80 mm/year. A seasonal pattern of displacements was observed, with higher rates during summer and autumn. The analysis suggested a remarkable influence of topographic conditioning factors for the identification of earth slide susceptibility, while lithology was more important for the identification of earth flow susceptibility. Limitations due to the widespread occurrence of landslides characterized by a complex style of activity and the yearly update schedule of the interferometric data used are acknowledged. Nonetheless, the proposed workflow demonstrates its replicability with minimal operational costs to assess landslide susceptibility and state of activity in diverse geomorphological contexts.

1. Introduction

Landslides are a natural process that encompasses both the sudden or gradual movement of debris, rock, and/or earth down a slope under the influence of gravity (Cruden and Varnes, 1996; Borgatti and Soldati, 2010; Crozier, 2010). While varying in their velocity of movement, these processes can pose a significant threat to human lives and livelihood, infrastructure, and cultural heritage (Lee and Jones, 2004; Glade and Crozier, 2005; Corominas et al., 2014; Micu et al., 2022). Landslide studies are not only fundamental to avoid potential life and economic losses (Crozier, 1986; Turner and Schuster, 1996; Glade and Crozier, 2005), but also to avoid the degradation and loss of value of culturally significant structures. Landslides are one of the main natural threats to the preservation of cultural heritage worldwide (UNESCO, 1972; UNESCO et al., 2010; ICOMOS, 2000, 2020; Bonini et al., 2023). Therefore, assessing landslide spatial and temporal frequency of occurrence is crucial when developing cultural heritage safeguarding strategies.

The first step of such a strategy can be a landslide susceptibility assessment. Landslide susceptibility is defined as the spatial probability of occurrence of a specific landslide type in a defined area (Brabb, 1984; Glade and Crozier, 2005). Susceptibility can be assessed using a wide

* Corresponding author at: Department of Chemical and Geological Sciences, University of Modena and Reggio Emilia, Modena, Italy.
E-mail address: carlotta.parenti@unimore.it (C. Parenti).

https://doi.org/10.1016/j.geomorph.2024.109522
Received 27 May 2024; Received in revised form 24 October 2024; Accepted 17 November 2024
Available online 20 November 2024

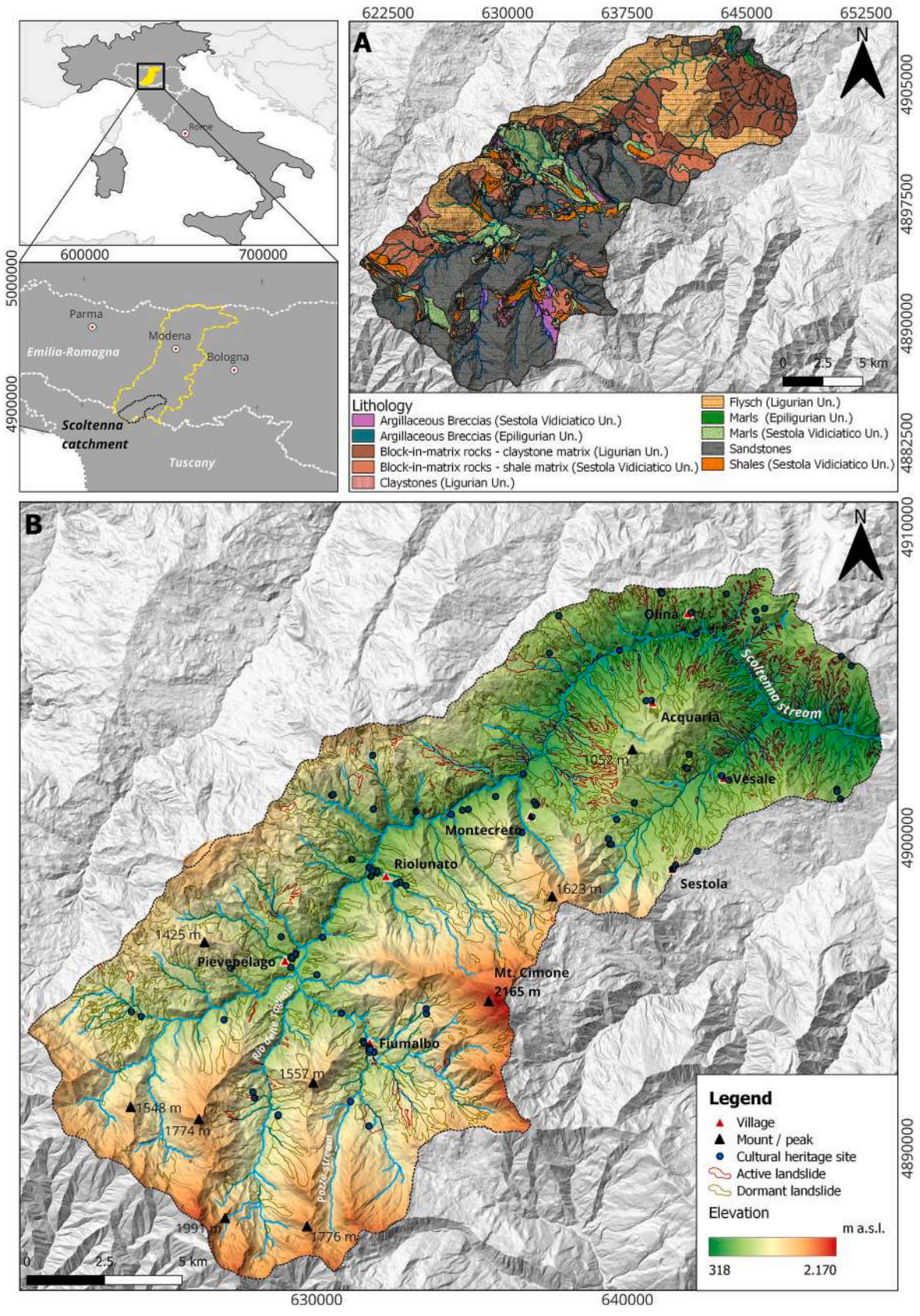

Fig. 1. Lithological map of the study area (A), and landslide state of activity and cultural heritage sites of the Scoltenna catchment (B).

range of methods whose selection should consider the project objectives, the mapping scale and size of the study areas, the environmental context, and the type of landslide under analysis (Soeters and van Westen, 1996; Guzzetti et al., 1999; van Westen et al., 2008; Hervás and Bobrowsky, 2009).

For large areas with complex geological and geomorphological settings, it is recommended to assess landslide susceptibility through data-driven models due to the spatial variability of soil and rock geotechnical properties that are key inputs for physically-based models (Carrara et al., 1991; Hervás and Bobrowsky, 2009; Corominas et al., 2014; Reichenbach et al., 2018). Several statistical methods have been deployed to assess landslide susceptibility, such as the information value (Yin and Yan, 1988; Jade and Sarkar, 1993; Chen et al., 2016; Bonini et al., 2020; El-Fengour et al., 2021), weights of evidence (Piacentini et al., 2012; Liberatoscioli et al., 2017; Barella et al., 2019), logistic regression (Ayalew and Yamagishi, 2005; Mancini et al., 2010; Zêzere et al., 2017; Broeckx et al., 2018; Chalkias et al., 2020), and generalized additive models (Petschko et al., 2014; Goetz et al., 2015; Steger et al., 2016, 2017; Brock et al., 2020). Machine learning algorithms, such as support vector machines (Pourghasemi et al., 2013; Hong et al., 2015; Chen et al., 2017) and Random Forest (Xu et al., 2012; Goetz et al., 2015; Pourghasemi and Rahmati, 2018; Zhou et al., 2021) have also been deployed in landslide susceptibility studies, and the interest in deep learning algorithms is growing (Sameen and Pradhan, 2019; Bui et al., 2020; Van Dao et al., 2020; Saha et al., 2023; Meng et al., 2024; Yang et al., 2024; Yu et al., 2024).

Statistically-based regional landslide susceptibility assessments aiming at identifying potentially affected cultural heritage sites are less common in literature, and some of them are not fully quantitative. Tarragüel et al. (2012) used spatial multicriteria decision analysis to assess landslide and avalanche susceptibility aiming at identifying possible adverse consequences to the cultural heritage of Upper Svaneti (Georgia). Klimeš (2013) assessed landslide susceptibility and frequency with a statistical approach at the Machu Picchu UNESCO World Heritage Site (WHS) and its surroundings. At the Matera archaeological area (Italy), Sdao et al. (2013) used neuro-fuzzy networks to identify critically susceptible areas. In Cyprus, Agapiou et al. (2015) identified natural and anthropogenic threats to the cultural heritage of Paphos District using the Analytical Hierarchy Process. Nicu (2018), Nicu and Asandulesei (2018) and Lombardo et al. (2020) produced landslide susceptibility maps using different statistical methods in the Moldavian Plateau, aiming to identify potentially threatened Cucuteni Neolithic sites. In the Honghe Hani UNESCO WHS (China), Jiao et al. (2019) mapped landside susceptibility through different data-driven methods, suggesting a method that could be replicated for other UNESCO sites. Kim and Kim (2021) overlapped cultural heritage site locations in the Chungcheong region (Korea) with a susceptibility map obtained through an ensemble of statistical and machine learning methods to select potentially threatened cultural heritage sites for future studies. In the Sikkim Himalayas (India), Saha et al. (2021) explored how changes in land use, landcover and rainfall regimes alteration due to climate change can impact debris and rock fall susceptibility, resulting in an increased exposure of cultural heritage to those landslide types. Yang et al. (2023) used a combination of methods on to evaluate, at the regional scale, the risk posed by different processes (including landslides) to the Yongtai Fortified manors (China). Potential natural and anthropogenic threats, including landslides, to the conservation of the ancient city of Ibb (Yemen) were assessed using a hybridized method AHP method by Dammag et al. (2024), revealing that most of the area is classified as high and very high risk of degradation. The majority of the mentioned regional scale studies were focused on establishing landslide spatial probability, with few examples that analyzed both landslide susceptibility and state of activity.

The growing availability of Earth Observation products and the advances in computing capabilities have not only made the gathering of information to perform data-driven landslide susceptibility analysis less time-consuming but also facilitated the monitoring of landslide state of activity over extensive areas. In particular, the use of spaceborne Synthetic Aperture Radars (SAR) for landslide detection and monitoring is promising due to their all-weather imaging capabilities and wide territorial coverage (Massonnet and Feigl, 1998; Wasowski and Bovenga, 2014; Mondini et al., 2021).

Multitemporal differential interferometry (MT-DInSAR) techniques allow the detection of terrain displacements achieving millimeter accuracy (Ferretti et al., 2001). In particular, Persistent Scatterer Interferometry (PSI) is one of the most widely-used MT-DInSAR techniques to obtain terrain displacement time series exploring the stable signal reflection of natural or built surfaces (Persistent Scatterers, henceforth referred to as PS) over a stack of multitemporal interferograms (Ferretti et al., 2001; Colesanti and Wasowski, 2006). PSI has been used to monitor volcanic activity (Hooper et al., 2004; Terranova et al., 2015; Wang et al., 2018), subsidence phenomena (Teatini et al., 2012; Raspini et al., 2014; Rosi et al., 2016; Amato et al., 2020; Mancini et al., 2021; Ng et al., 2023; Qiao et al., 2023; Wu et al., 2023; Zhou et al., 2024), and displacements due to slow and very-slow moving landslides (Colesanti and Wasowski, 2006; Bianchini et al., 2013; Notti et al., 2014; Wasowski and Bovenga, 2014 Piacentini et al., 2015; Ciampalini et al., 2016a, 2016b; Mantovani et al., 2016; Carlà et al., 2019; Cignetti et al., 2023).

MT-DInSAR have been previously used to identify and characterize potential landslide effects on cultural heritage sites. Gigli et al. (2012) integrated detailed geological mapping, geomechanical survey, terrestrial laser scanner surveys, numerical and kinematic analysis, and PSI to investigate the instability mechanisms of the Mdina bastions and the Citadel sites of the Maltese Islands. The PROTection of European Heritage from GeO-hazards (PROTEGHO) project low-impact multiscale method combined MT-DInSAR and other geomatic survey techniques aiming to diagnose the situation of cultural heritage sites and support safeguarding strategies (Themistocleous et al., 2016, 2017, 2021). The PanGeo methodology is another example, as demonstrated by Cigna et al. (2015) in the study of the Greater London metropolitan area. The potential to produce a priority list of hazardous zones that demand attention in cultural heritage sites based on MT-DInSAR is further demonstrated by Pastonchi et al. (2018) at the regional scale for the UNESCO World Heritage Sites of Tuscany (Italy). Using MT-DInSAR and in situ geomatic surveys, Reale et al. (2019) assessed the potential structural effects of slow-moving landslides in the St. Gerlando Cathedral (Agrigento, Italy). Most studies deploying MT-DInSAR aimed at characterizing the state of activity and/or the displacements effects on built structures over extensive areas. However, studies that also provided information on landslide spatial probability are less common, and this type of information could be useful for cultural heritage management and related decision-making processes.

In this paper, we aim to fill the gap for a regional scale landslide susceptibility and state of activity analysis for identifying potentially affected built environments. The paper outlines an open-source and quantitative workflow for such purpose. The workflow integrated data-driven landslide susceptibility mapping and MT-DInSAR, and was tested to identify cultural heritage sites that can be affected by landslides in a catchment located in the Northern Apennines (Italy).

2. Study area

The Scoltenna stream catchment (approximately 280 km^2) is located in the Modena Apennines (Fig. 1), Emilia-Romagna Region, Northern Italy. The main geological units of the Modena Apennines are represented by the Tuscan Unit (composed of siliciclastic deep-water turbidites), the Ligurian Unit (deep-sea oceanic sediments with Jurassic ophiolites covered by calcareous terrigenous turbidites), the unconformably overlying Epi-Ligurian successions (mainly terrigenous sediments), and the Plio-Eocene marine-terrigenous deposits that rest unconformably over the Epi-Ligurian and Ligurian units (Bertolini et al., 2005). Hinterland-to-foreland propagating thrusts, folds and faults were

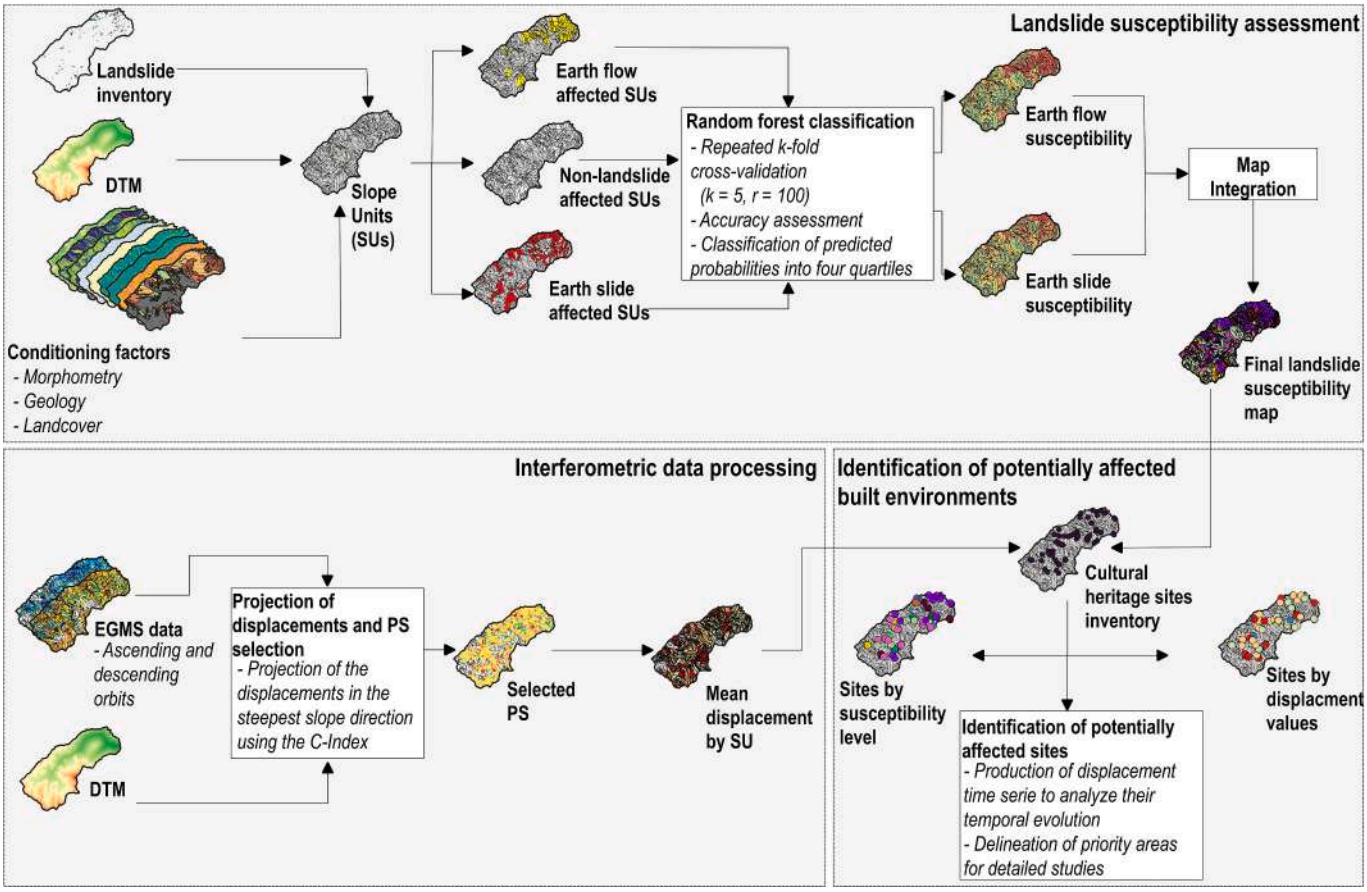

Fig. 2. Workflow of the proposed approach.

developed during the collisional event when the tectonic units belonging to the oceanic domain (Ligurian Domain) and the epicontinental margin (Tuscan Domain) were transported to the east (Carosi et al., 2004).

The sedimentary marine rocks originated mostly in a period between the Lower Cretaceous and the Upper Pliocene were raised and deformed during the orogenic phases that led to the current structure of the Northern Apennines. The geology of the study area can be summarized as a heterogenous alternation of prevalently clayey layered rock types (in the south of the Scoltenna catchment) with intensely fractured sandstones and limestones (mainly in the northern sector of the catchment) (Abbate et al., 1970; Piacentini et al., 2018).

In the Scoltenna catchment, the slopes are prone to landslide processes because of the physical weathering of the geological formations, the decay of mechanical properties, and the progressive water absorption (Bertolini et al., 2002; Bertolini et al., 2005). The landforms occurring in the catchment are the result of a series of morphogenetic processes generally linked to lithological-structural factors, climatic conditions, and anthropic activities (Soldati, 1997). The prevalent clayey nature of the rocks, their tectonization, intense and/or prolonged rainfall contribute to the occurrence of slope movements of various types, sizes and ages. The landslide types are essentially conditioned by the mechanical characteristics of the geological formations. Landslides due to flow are typical of the predominantly clayey soils which, soaked in by precipitation waters, give rise to plastic-viscous movements (Tosatti, 1982; Cancelli et al., 1987). The most frequent landslide types in the study area are dormant and active earth slides and flows (Bertolini and Pellegrini, 2001; Ronchetti et al., 2007; Castaldini et al., 2012; Bertolini et al., 2017; Mulas et al., 2018; Piacentini et al., 2018; Parenti et al., 2023).

Rainfall is the main landslide trigger in the Scoltenna catchment, with a secondary contribution of snowmelt and rare cases in which earthquakes played a central role in landslide triggering (Castaldini et al., 2012; Bertolini et al., 2017; Piacentini et al., 2018). Rainfall pattern is orographically influenced, and the average total annual precipitation is 1,227 mm in the lower Scoltenna catchment and 1,902 mm in the upper Scoltenna catchment (data recorded in the period 1954–2022) (https://www.arpae.it/). The climate of the area is classified as "sub-continental" and locally as "cool-temperate" with a mild temperate climate (Cfa) (Köppen, 1931).

3. Materials and methods

Our approach for the identification of potentially landslide-affected built environments can be summarized in three steps (Fig. 2): a) Landslide susceptibility assessment, performed independently for each landslide type, and then integrated in a synthetic map; b) Analysis of open and free interferometric products and reprojection of the line of sight velocities to the steepest slope direction; and c) ranking of the cultural heritage sites by their susceptibility level and displacement values, with the analysis of the temporal evolution of displacements.

3.1. Landslide susceptibility maps

Landslide location, type, style of activity, and state of activity were retrieved from the Italian Landslide Inventory (IFFI) freely available for the whole country at the ISPRA Idrogeo platform [https://idrogeo.isprambiente.it/app/iffi] (Trigila et al., 2010; Iadanza et al., 2021). Landslide state of activity registered in the IFFI is based on direct field evidence, archive data, aerial photo interpretation, and radar interferometry. A given landslide is defined as dormant if it has not experienced a reactivation event in the last year. The rationale of the one year-threshold is that during one year a slope is subject to one or more wet seasons, and a

Table 1
Selected landslide conditioning factors and their data sources.

Conditioning factor		Data source
Morphometric	Slope (mean and σ)	DTM of the Emilia-Romagna region (5 m res.)
	Profile curvature (mean and σ)	DTM of the Emilia-Romagna region (5 m res.)
	Planar curvature (mean and σ)	DTM of the Emilia-Romagna region (5 m res.)
	Northness (mean and σ)	DTM of the Emilia-Romagna region (5 m res.)
	Eastness (mean and σ)	DTM of the Emilia-Romagna region (5 m res.)
	Topographic Wetness Index (mean and σ)	DTM of the Emilia-Romagna region (5 m res.)
	Convergence Index (search radius = 10 cells) (mean and σ)	DTM of the Emilia-Romagna region (5 m res.)
	Convergence Index (search radius = 50 cells) (mean and σ)	DTM of the Emilia-Romagna region (5 m res.)
	Flow accumulation (log-scale) (mean and σ)	DTM of the Emilia-Romagna region (5 m res.)
Geological	Lithology (% of SU covered by each class)	Geological maps of the Emilia-Romagna and Tuscany regions (1:10.000 scale)
Landcover	Landcover (% of SU covered by each class)	Corine Landcover Plus (10 m)

period of snowmelt in certain Italian regions, which may cause landslide reactivation (Pasuto and Soldati, 1996; Borgatti and Soldati, 2005; APAT, 2004) A total of 424 landslide polygons are classified as active in the Scoltenna catchment according to the IFFI (182 earth slides, 117 earth flows, 81 with complex style of activity, 40 of undetermined type, and 4 rock fall source areas). Active landslides correspond to 11.22 km^2 of the catchment (approximately 4% of the total area).

The conditioning factors data for the landslide susceptibility models were derived from different data sources and can be grouped into three categories: morphometric, lithological, and landcover (Table 1). Slope Units (SU) were employed as the cartographic unit for the landslide susceptibility assessment. SU derivation is based on drainage and ridge lines and can be considered more geomorphologically accurate than the traditional, arbitrarily sized, grid-based approach for regional susceptibility assessments (Carrara, 1983; Guzzetti et al., 1999). SU partition was obtained from the DTM using the Slope Unit Maker version 1.1.3 (SUMak), recently introduced by Woodard et al. (2024). The SU mean and standard deviation of morphometric conditioning factors were derived, while for the other types of conditioning factor the percentage of SU area covered by each class was considered, totaling 20 independent input features for the susceptibility model (Table 1).

Slow-moving earth slides and earth flows are the predominant landslide processes in the Scoltenna catchment as shown by Parenti et al. (2023). In this paper, we considered that earth slides and the less frequent block slides that occur in the upper part of the catchment could be merged into a single class for the susceptibility model. A similar simplification was deployed for the earth flows partially covered with rock falls deposits, but in this case, rock falls were not considered in the model, being flow assumed as the dominant landslide mechanism. We used this categorization due to the prevalence of earth slides and earth flows in the study area, with the aim to outline the most susceptible terrains on a catchment scale.

In the IFFI landslide inventory, some of the mapped landslides display a complex style of activity according to Cruden and Varnes (1996), while others were classified as of undetermined type. To include those landslides in our modeling framework, we reclassified the complex and undetermined type landslide polygons based on two criteria (Fig. 3).

Given the different kinematics of earth flows and earth slide processes, the susceptibility to each one of those processes was assessed independently through a Random Forest (RF) machine learning algorithm (Breiman, 2001), a non-parametric technique based on an ensemble of decision trees. Two independent RF classifications were trained using 500 trees with maximum tree depth equal to 7. Different tree depths were tested to evaluate the effect of tree depth on accuracy. The value was selected in a preliminary step and the selection aimed to maximize accuracy while also avoiding deeper trees that could lead to model overfitting. Accuracy was assessed using repeated k-fold cross-validation (Kohavi, 1995), resulting in 500 estimates of classifications' accuracy (100 repetitions of 5-fold cross-validation) for each landslide type. Model accuracy was assessed through the Area Under Curve (AUC)

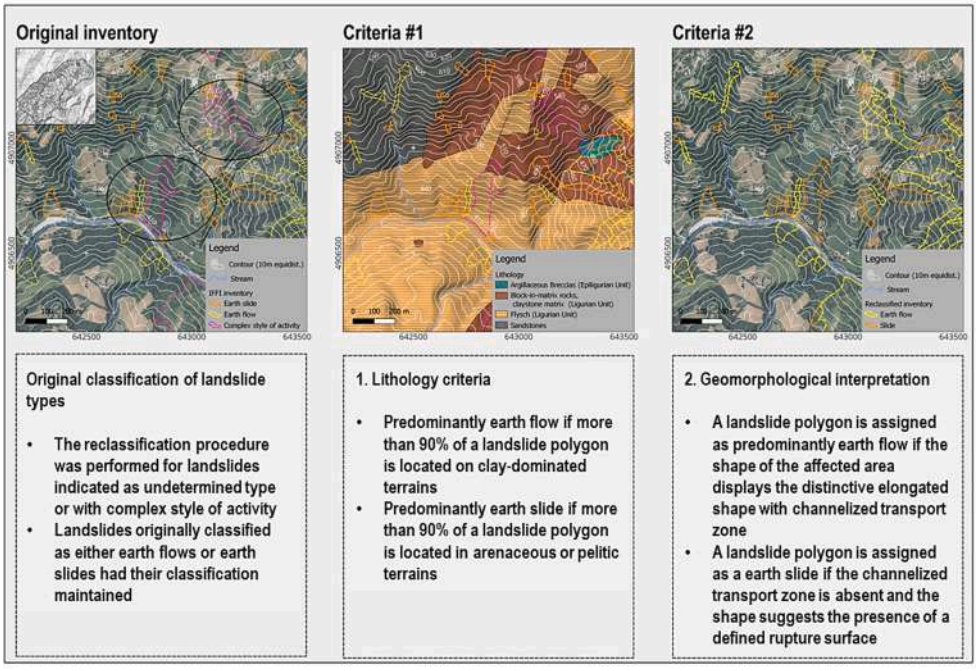

Fig. 3. Procedure used to reclassify the undetermined type landslides and the ones with complex style of activity, based on lithology and geomorphological interpretation criteria.

Table 2
Cultural heritage sites by category and epoch as registered in the Emilia-Romagna WebGIS database.

Site category	Number of sites	Epoch				
		Not indicated	Medieval	Renaissance	Modern	Contemporary
Bridge	10	1	1	3	1	4
Religious building	52	5	10	12	18	7
Graveyard	12	12	0	0	0	0
Landmark	3	0	0	1	1	1
Residential Building	5	2	0	2	0	1
Fortress	6	1	3	1	0	1
Civil structure	3	0	0	0	1	2
Windmill	1	0	0	1	0	0
Total	92	21	14	20	21	16

of the Receiver Operating Characteristics (ROC) curve (Bradley, 1997; Fawcett, 2006), which was computed for each test fold and summarized by its Interquartile Range (IQR) across all repetitions. A SU was used as a landslide sample for the RF classification if it contained a landslide register in the IFFI inventory (141 earth flow affected SUs and 145 earth slide affected). An equal number of non-landslide-affected SUs were randomly selected for the application of the RF classifier.

Conditioning factor importance for each of the classifications was assessed through the mean decrease in the Gini coefficient. This metric indicates how much a variable contributes to the separation of tree nodes containing mixed labeled elements (i.e., landslide and non-landslides) into single-class nodes (Han et al., 2016). The higher the value assumed by the mean decrease in the Gini importance coefficient, the higher the usefulness of the variable for the classification (Han et al., 2016).

The best-performing RF models were used to separately estimate earth flow and earth slide spatial probabilities across all SUs. Finally, to combine the maps, the prediction probabilities for each landslide type were classified into four quartiles, from low to high susceptibility. The reclassified maps were then combined in a map with 16 unique classes from low (S1-F1, which indicates low susceptibility both to earth slides and earth flows) to high (S4-F4). The combination was carried out following Lombardo et al. (2020) approach to combining SU-based landslide and gully erosion susceptibility maps by map algebra.

The R open-source software (R Core Team, 2019) performed all processes described in this section: conditioning factor data processing using the *rsagacmd* package (Pawley, 2023), deploying the *SUMak* R-code, and RF training and prediction using the *caret* package (Kuhn, 2008).

3.2. Landslide susceptibility and state of activity at cultural heritage sites

The location of cultural heritage sites in the study area was extracted from the online platform curated by the Regional Secretariat for the Emilia-Romagna Region (https://www.patrimonioculturale-er.it/webgis/), a catalog compiled by the regional authority as part of the response efforts to the damages resulting from the Emilia-Romagna 2012 earthquake. The database was queried for the architectonic and archaeological sites of cultural significance at national and regional levels.

A total of 92 architectonic sites and zero archaeological sites were identified in the study area (Table 2). The sites were built between the Medieval epoch and the XX century, mostly ecclesiastic properties such as churches, monasteries, and chapels. Several cultural heritage sites are located in the vicinity of dormant and active landslides according to the IFFI (Fig. 1). However, the database does not provide information about the state of conservation of the sites and the potential adverse consequences of natural and human-induced processes.

To analyze the landslide state of activity in SUs containing cultural heritage sites we used PSI data provided by the European Ground Motion Service (EGMS) (Table 3). The EGMS calibrated dataset consists of PSI derived from Sentinel 1 data from 2015 to 2021 and is made available for the territory of all European Union members as part of the

Table 3
Statistics of the interferometric data from 2016 to 2021.

	Geometry	
	Ascending	Descending
Temporal coverage	10-02-2015 to 23-12-2021	15-04-2015 to 27-12-2021
Number of PS	36,802	32,623
PS density (PS/km^2)	130.26	115.39
Mean V_{LOS} (mm/year)	−2.65	−1.81
Maximum positive V_{LOS} (mm/year)	10.6	11.6
Minimum negative V_{LOS} (mm/year)	−20.9	−20.7

Copernicus Land Monitoring Services. Calibrated EGMS products are referenced using data from GNSS stations spread across the European continent and contain no assumptions regarding the direction of the terrain displacements (Crosetto et al., 2020; Crosetto and Solari, 2023).

The ground displacement velocities measured along the radar's Line of Sight (V_{LOS}) for the ascending and descending orbits were combined after reprojecting the V_{LOS} in the steepest slope direction (V_{slope}) using the C-index (Cascini et al., 2010; Notti et al., 2014). The C-index amounts to the percentage of displacement measured by the radar and can be obtained with Eq. (1), which requires: a) the directional cosines of the sensor LOS during data acquisition (N, E, and H); and b) slope (s) and aspect (a), derived from the DTM. After computing the C-index for each PS, the V_{slope} values can be calculated through Eq. (2) (Cascini et al., 2010; Notti et al., 2014).

$$C = \{N\cdot[-cos(a)\cdot cos(s)]\} + \{E\cdot[-1\cdot sin(a)\cdot cos(s)]\} + [H\cdot sin(s)] \quad (1)$$

$$V_{slope} = \frac{V_{LOS}}{C} \quad (2)$$

The computation of V_{slope} using the C-index can result in a potential bias due to the assumption that the direction of movement is the steepest slope direction when projecting V_{LOS}. Aiming to mitigate this bias, a PS selection procedure was used (Bianchini et al., 2013; Herrera et al., 2013; Notti et al., 2014; Cignetti et al., 2023): a) Exclusion of PS with C-index value inside the range [−0.2, 0.2], that indicate an overestimation of V_{slope} resulting from the projection along the slope direction; b) Removal of PS in areas with slope gradient under 5°, due to projection exaggeration and to possible detection of subsidence movements and c) PS with velocities >+2 mm/year were discarded since they are not geomorphologically reasonable for landslide studies (e.g., a landslide moving upslope). The deployed PS selection procedure results in a reduction of the PS population.

PSI data was integrated with the SU-based susceptibility map by computing the mean of the V_{slope} modulus for each SU containing three or more PS. Then, for each cultural heritage site, the susceptibility level and the SU mean V_{slope} modulus were retrieved and analyzed aiming to identify the sites that could be affected by active landslides. Moreover, we selected a cultural heritage site located in an SU classified as one of

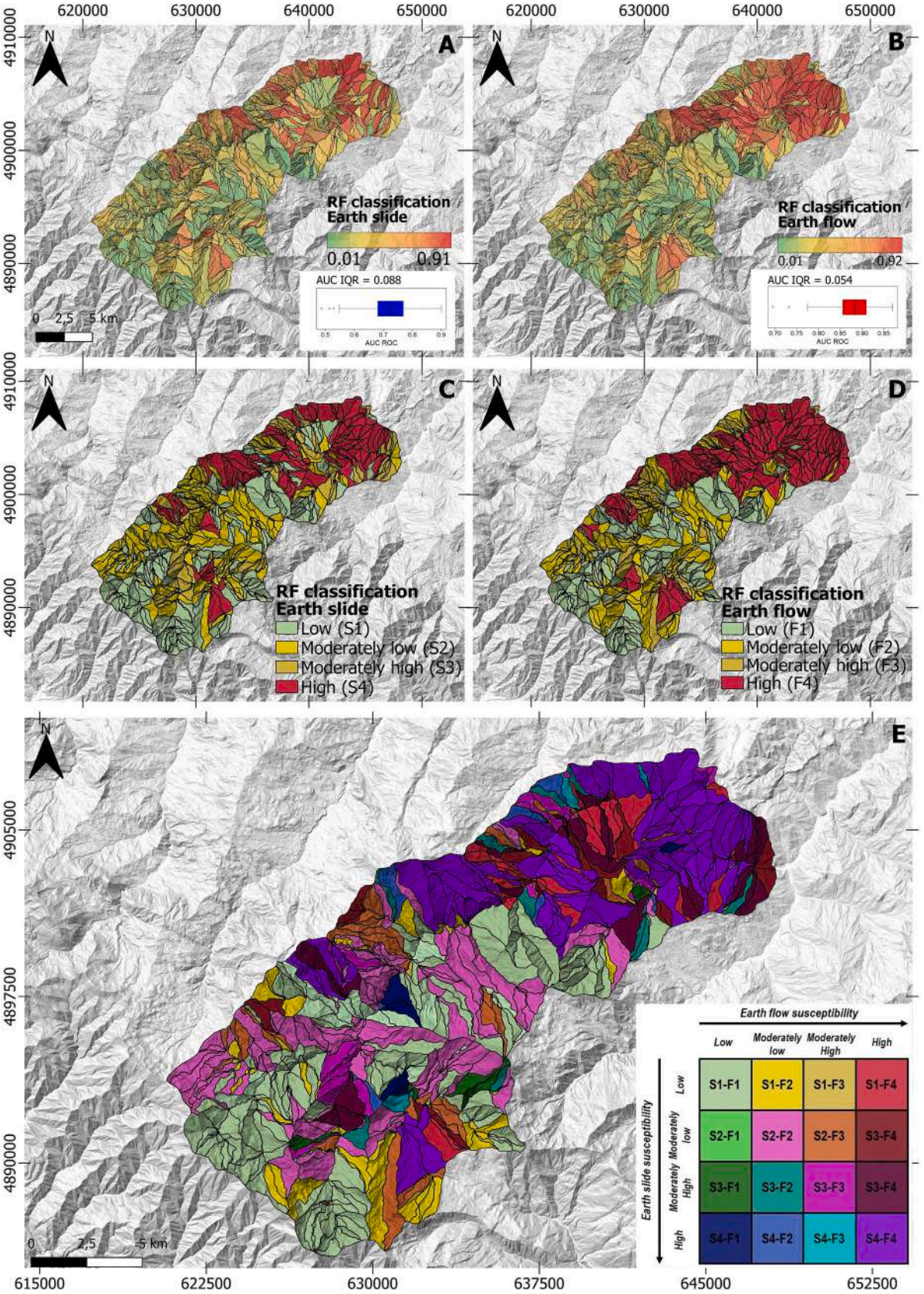

Fig. 4. Prediction probabilities for earth slide (A) and earth flow (B) landslide types; Reclassified susceptibility map into four quartiles for earth slide (C) and earth flow (D); and the result of the combination of the reclassified susceptibility maps into a susceptibility map with 16 classes (E).

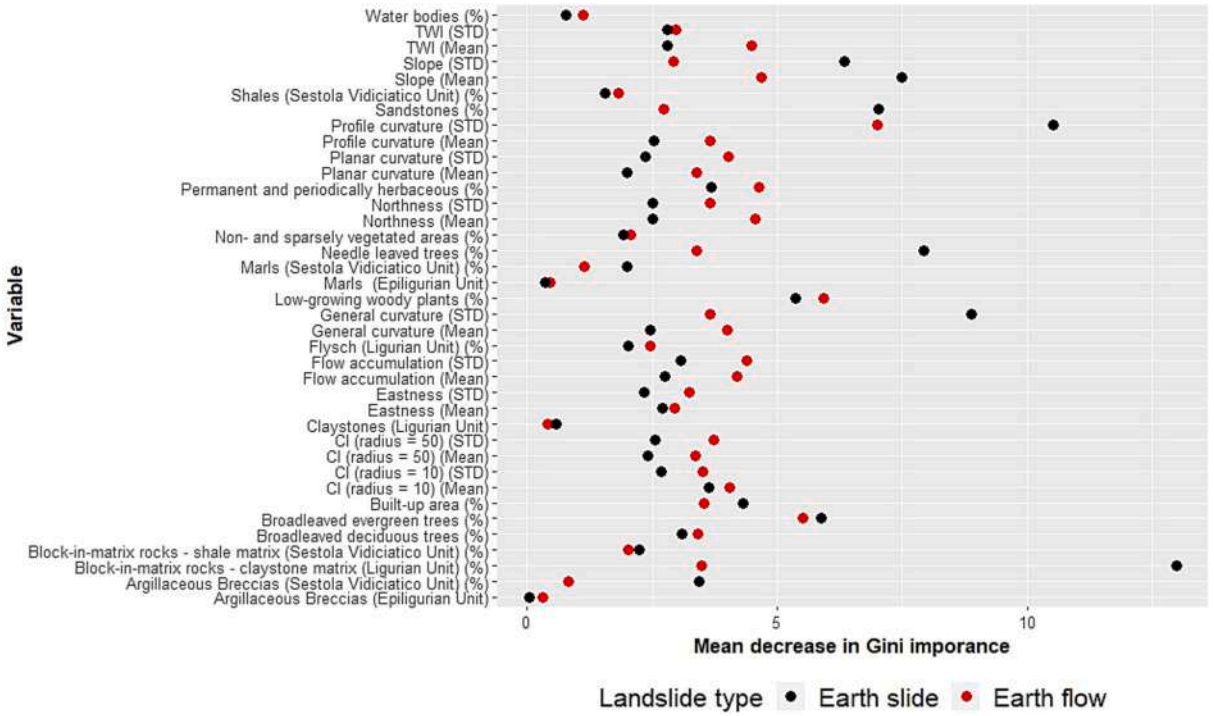

Fig. 5. Random Forest classification conditioning factor importance for the earth slide susceptibility model and the earth flow susceptibility model.

the most susceptible and one of the higher displacements as a case study. In the case study, the displacement values provided in the EGMS dataset for each image acquisition were summarized yearly and on a seasonal basis to assess the temporal evolution of displacements and the presence of seasonal behaviors. For the seasonal mean displacement computation, we considered the astronomical seasons for the northern hemisphere (e.g., defined by the solstices and equinoxes).

4. Results

4.1. Landslide susceptibility maps

Based on the cross-validation results, the earth slide and earth flow susceptibility models have high predictive performances, with median AUC ROC values of 0.72 and 0.88, respectively. The best-performing models achieved AUC ROC values of 0.90 and 0.97 for the earth slide and earth flow models, respectively. The susceptibility models also show high robustness and stability in the predictions, with AUC ROC interquartile ranges under 0.10 for both susceptibility models (0.088 for the earth slide model and 0.054 for the earth flow model) The parameters of the best-performing models were used to estimate earth slide and earth flow spatial probabilities across all SUs (Fig. 4A and B).

The reclassified maps into four quartiles (Fig. 4C and D) were combined into a susceptibility map with 16 classes (Fig. 4E). In the susceptibility map, one can notice that the lower sector of the Scoltenna stream catchment is highly susceptible to both landslide types, but mainly to earth flows. In the lower Scoltenna catchment, some north-facing SUs are depicted as highly susceptible to earth flows and with low susceptibility to earth slides (S1-F4 in the susceptibility map). This shows that the Random Forest classifier was able to capture the individual contributions of the conditioning factors to the occurrence of each particular landslide type, despite being trained with the same set of conditioning factors.

Conditioning factor importance show that morphometric properties of the SUs related to hydrology (e.g., flow accumulation, convergence index, planar and profile curvature, and TWI) are more significant to the earth slide model than they are for the earth flow model (Fig. 5). On the other hand, most of the lithological classes are more meaningful for the earth flow model. Moreover, for the earth flow model, there is a tendency for the standard deviation of the morphometric variables for the SU to be more relevant than the mean value for the SU.

4.2. Persistent Scatterer Interferometry (PSI)

The PSI analysis shows that most of the Scoltenna stream catchment is affected by displacements that can be caused by landslides (Fig. 6A and B), although most of it shows slow V_{LOS}. After the computation of V_{slope}, for a population composed of 69,425 PS (36,802 from ascending orbit and 32,623 from the descending orbit) the following number of PS was discarded in each step of the selection procedure: a) 17,013 PS based on the C-index threshold; b) 6823 based on the slope angle threshold; and c) 6000 PS based on the V_{slope} threshold. The PS population was reduced by 43% (Table 4). The relatively high number of discarded PSs could be the result of the presence of a significant number of shallow slopes and the uncertainty related to the DTM heights and the resolution of the DTM that could affect the estimation of the slope inclination value. Nevertheless, the PS population for the combined orbits (Fig. 6C) still has a density of approximately 141 PS/km^2 considering the total catchment area a mean of 226 PS/km^2 by SU. Nearly 27.5% (n = 172) of the SUs were discarded due to a low PS population (<3 PS) (Table 4).

4.3. Cultural heritage sites potentially affected by landslides

The Scoltenna catchment cultural heritage sites are spread all over the area, except for the uppermost zone of the catchment characterized by higher elevations and steeper slopes of the Northern Apennines that mark the border between the Emilia-Romagna and Tuscany regions (Fig. 7). Most of the sites (52) fall into the low to moderately low susceptibility classes for both processes (S1-F1 to S2-F2) (Fig. 7) and PSI data shows that the majority of the SUs where these sites are located display 1st and 2nd quartile mean displacement values for the period 2015–2021. Most of those sites are bridges, religious buildings, and residential buildings located in SUs containing dormant landslides along

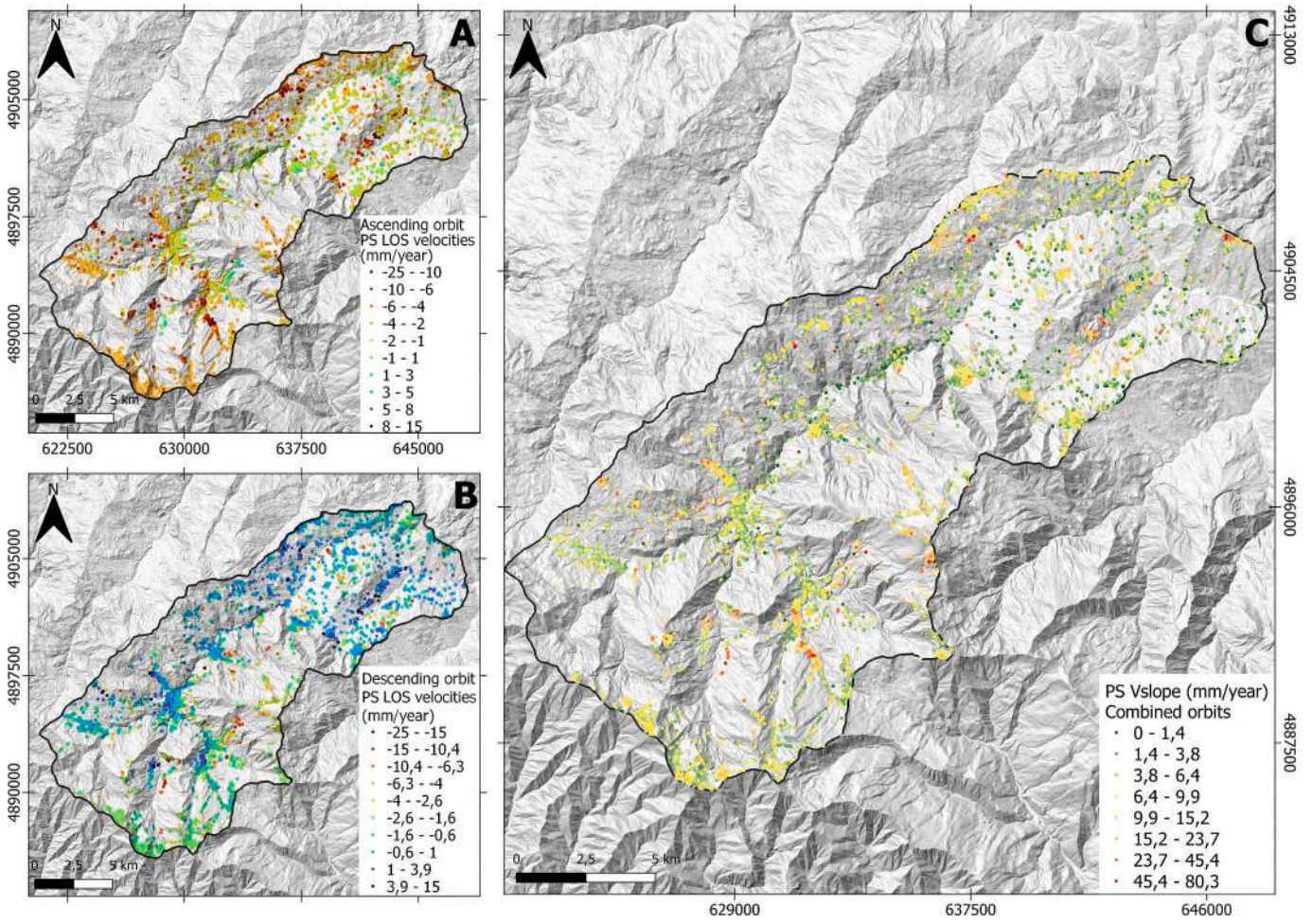

Fig. 6. PSI data coverage in the study area. (A) PS ascending orbit mean Line of Sight Velocities (V_{LOS}) for the Sentinel-1 time series; (B) PS descending orbit mean V_{LOS}; and (C) Results of the V_{LOS} projection to the local steepest slope direction and computation of its modulus, resulting in V_{slope}.

Table 4
Statistics of the interferometric data after the reprojection along the steepest slope.

	Geometry		
	Ascending	Descending	Ascending + Descending
Number of selected PS	20,575	18,974	39,549
Selected PS density (PS/km^2)	73.482	67.764	141.246
Mean of selected PS density by SU area (PS/km^2)			226.405
Maximum negative V_{slope} (mm/year)	−80.269	−76.498	−80.269
Mean V_{slope} (mm/year)	−6.183	−4.424	−5.339
Number of Slope Units with >3 PS			453
Number of no data Slope Units (<3 PS)			172
Mean selected PS population by SU			87.220
Slope Unit maximum mean V_{slope} module (mm/year)			15.347
Slope Unit minimum mean V_{slope} module (mm/year)			1.462
Slope Unit mean of mean V_{slope} module (mm/year)			5.703

the course of the Scoltenna stream. Only one of the fortresses of the catchment is located in an SU characterized by a low susceptibility level (S1-F2) but with mean displacement in the 3rd quartile of values (Fig. 7).

On the other end of the susceptibility classification, 18 cultural heritage sites are located on SUs with the highest susceptibility to both landslide types (S4-F4), most of them also religious buildings, bridges, graveyards, and fortresses. Out of the 18 sites, 5 show mean displacement values on the time series in the 4th quartile (Fig. 7), mainly bridges and fortresses. The high susceptibility level of the SUs containing fortresses can be associated with the topographic position of those structures, usually constructed on hilltops that provide a strategic viewpoint for military purposes. On the other hand, bridges with high displacement levels, such as the Medieval Olina Bridge (Fig. 8), have their displacement associated with other structural deformations since there is no field evidence of landslides affecting this structure.

To exemplify our approach, we selected two cultural heritage sites in the highest susceptibility class to both processes: the Gaiato Tower (Fig. 9A) and the Sacra Famiglia oratory (Fig. 9B). The tower is the last remnant of a fortress built in the XII century and stands on a hilltop (926 m) close to the crown of a landslide of complex style of activity whose first description dates to the XVII century and is named after the Gaiato locality in the lower sector of the catchment (Tosatti, 1982).

The nearly 3 km long accumulation zone of the Gaiato landslide moves mainly due to earth flows on the clay terrains of the Chaotic complex. This mechanism can lead to rock falls and block slides detaching from the sub-vertically fractured calcarenites of the

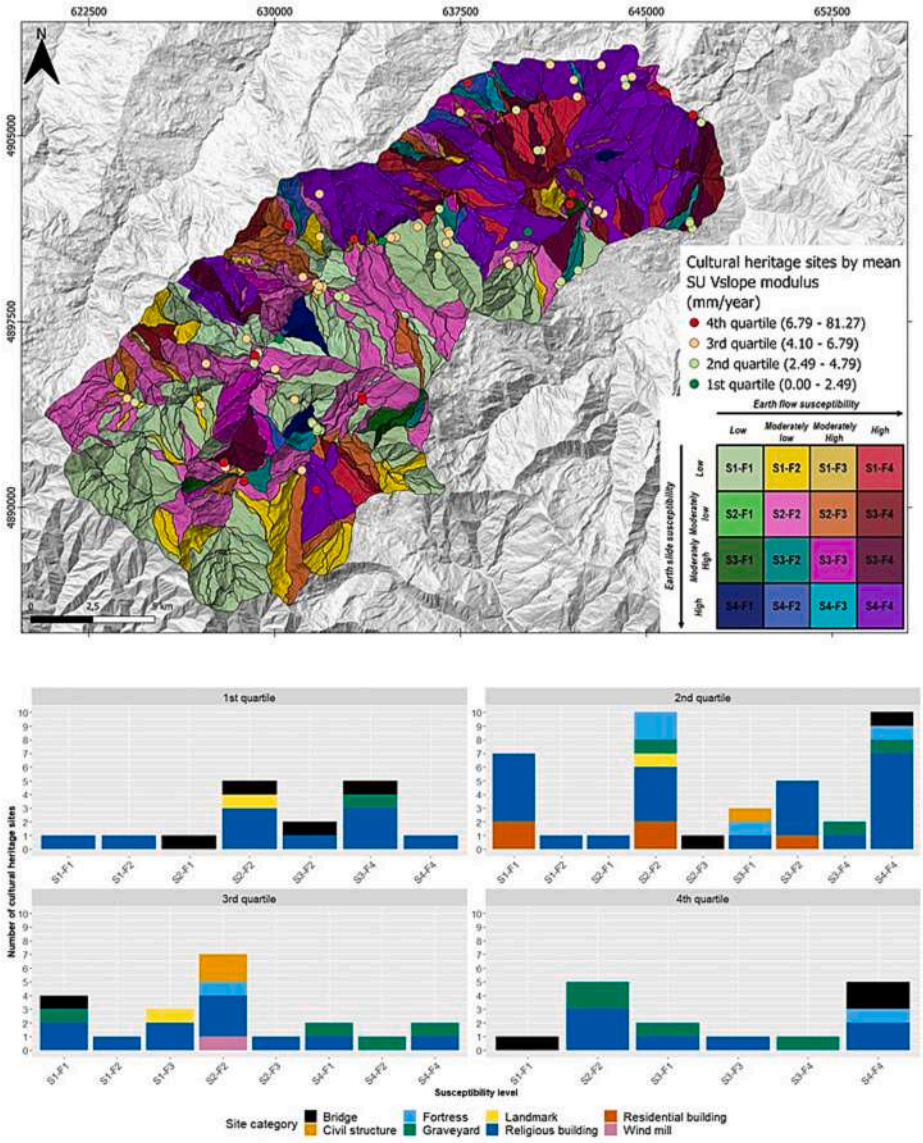

Fig. 7. Cultural heritage sites of the Scoltenna catchment, color-coded by SU V_{slope} quartiles and superimposed to the susceptibility map. Graph with site category according to the susceptibility level and SU mean displacement quartiles.

Bismantova Formation (Gelmini and Pellegrini, 1969; Tosatti, 1982). Moreover, the upper part of the landslide is registered in the official landslide inventory as a deep-seated gravitational slope deformation (Iadanza et al., 2021). The reactivation of a deep rupture surface is associated with the infiltration of rainfall in the fracture networks of the Bismantova Formation, eventually reaching the less permeable clay formations underneath (Gelmini and Pellegrini, 1969; Tosatti, 1982). The most recent movements occurred after intense rainfall between March and April 2013.

The Sacra Famiglia oratory is located in the upper sector of the Scoltenna catchment (1,188 m), in the Faidello fraction of the Fiumalbo municipality. The small oratory was built in 1845 and is the main reference point of the village. The whole village stands on top of an active landslide with complex style of activity, mainly due to a slow-moving earth flow mechanism, with a total area of approximately 320,000 m^2 as registered in the IFFI. The area is located in the higher zones of the catchment and is characterized by the contact between three lithologies: block-in-matrix rocks with shale matrix (Sestola-Vidiciatico unit); Macigno Formation sandstones; and argillaceous breccias (Sestola-Vidiciatico unit).

Interferometric data for the Gaiato SU (Fig. 10A and C) show two displacement episodes and a tendency to higher displacement values during autumn and summer (Fig. 10C). During the first episode, the mean annual displacement increased from approximately 1.6 mm in 2015 to nearly 5.5 mm in 2018, with a mean displacement of 5.5 mm during the summer of 2018 (Fig. 10C). From 2018 to 2020, the mean annual and seasonal displacements remained relatively stable at around 5.8 mm/year (Fig. 10C). The second acceleration episode takes place from 2020 to 2021 (the last year in the interferometric time series) and shows a significant increase in the displacement rate (up to approximately 7.8 mm during the summer of 2021).

PSI analysis revealed that the Oratory SU displayed a consistent increase in the displacement rates in the period 2015–2021 (Fig. 10B and D). In 2015, the mean displacement was 7.8 mm and the area has experienced a sharp increase from 2016 onwards, with a mean value of 77.4 mm in 2021. The same seasonal displacement pattern observed in the Gaiato Tower SU could be observed in the oratory SU. Mean seasonal displacement tend to be higher during autumn and summer, respectively 82.8 mm and 78.2 mm in 2021.

Fig. 8. The Olina Bridge during filed surveys in May 2023 when it was being repaired due to the increase in the number of cracks in the structure.

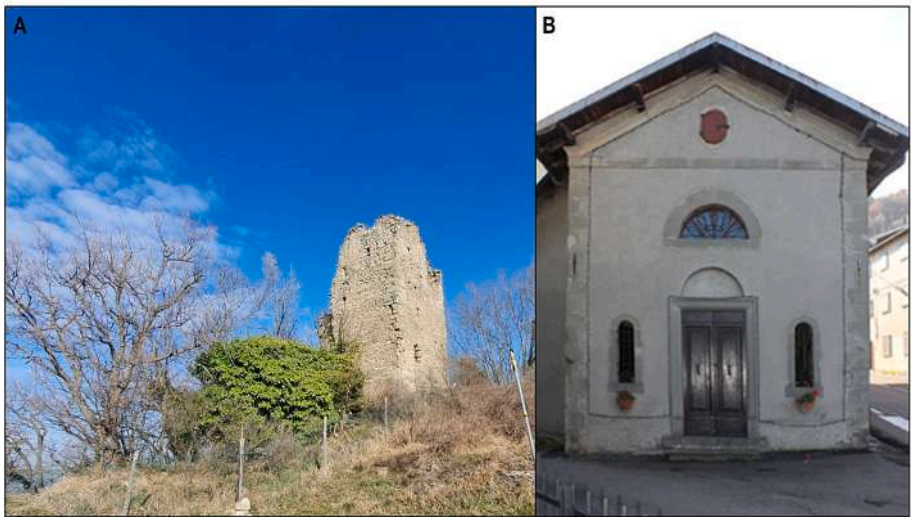

Fig. 9. The Gaiato tower in the lower sector of the Scoltenna catchment (A); and the Sacra Famiglia oratory in the Fiumalbo municipality (B). Source: Ufficio Nazionale per i beni culturali ecclesiastici e l'edilizia di culto (B).

5. Discussion

The susceptibility modeling resulted in reasonably accurate predictions for the identification of areas prone to earth slides and earth flows at the regional level. Previous studies in the area were mainly focused on the analysis of specific landslides (Gelmini and Pellegrini, 1969; Tosatti, 1982) and the coupling between fluvial and slope dynamics (Parenti et al., 2023). Landslide susceptibility mapping results showed: a) that the standard deviation of morphometric parameters can better depict the SU morphometric variability related to the large earth flow affected areas, while the mean is more useful to identify the smaller earth slide affected areas; and b) in the study area, earth slides are mainly topographically controlled, whereas lithological controls are more relevant for earth flow susceptibility.

The standard deviations of morphometric parameters allow to capture the variability of the terrain morphometry across the slope unit. Thus, its stronger relation with earth flows can be associated to a better representation of the geomorphological variability of the terrain that determines the occurrence of such landslides in the study area. This finding suggests that the use of more statistical measures in susceptibility models can help researchers to identify different relationships between landslides and their conditioning factors. Future research can select critical areas for detailed studies aiming to explore the aforementioned relationships between different landslide types and conditioning factors in other areas of the Modena Apennines.

The integration of the susceptibility map with interferometric data allowed us to identify two sites in the highest susceptibility class to both landslide types and with concerning displacement rates in the period 2015–2021. Additionally, the seasonal analysis of the displacement time series for the Gaiato Tower and Oratory SUs shows that faster mean

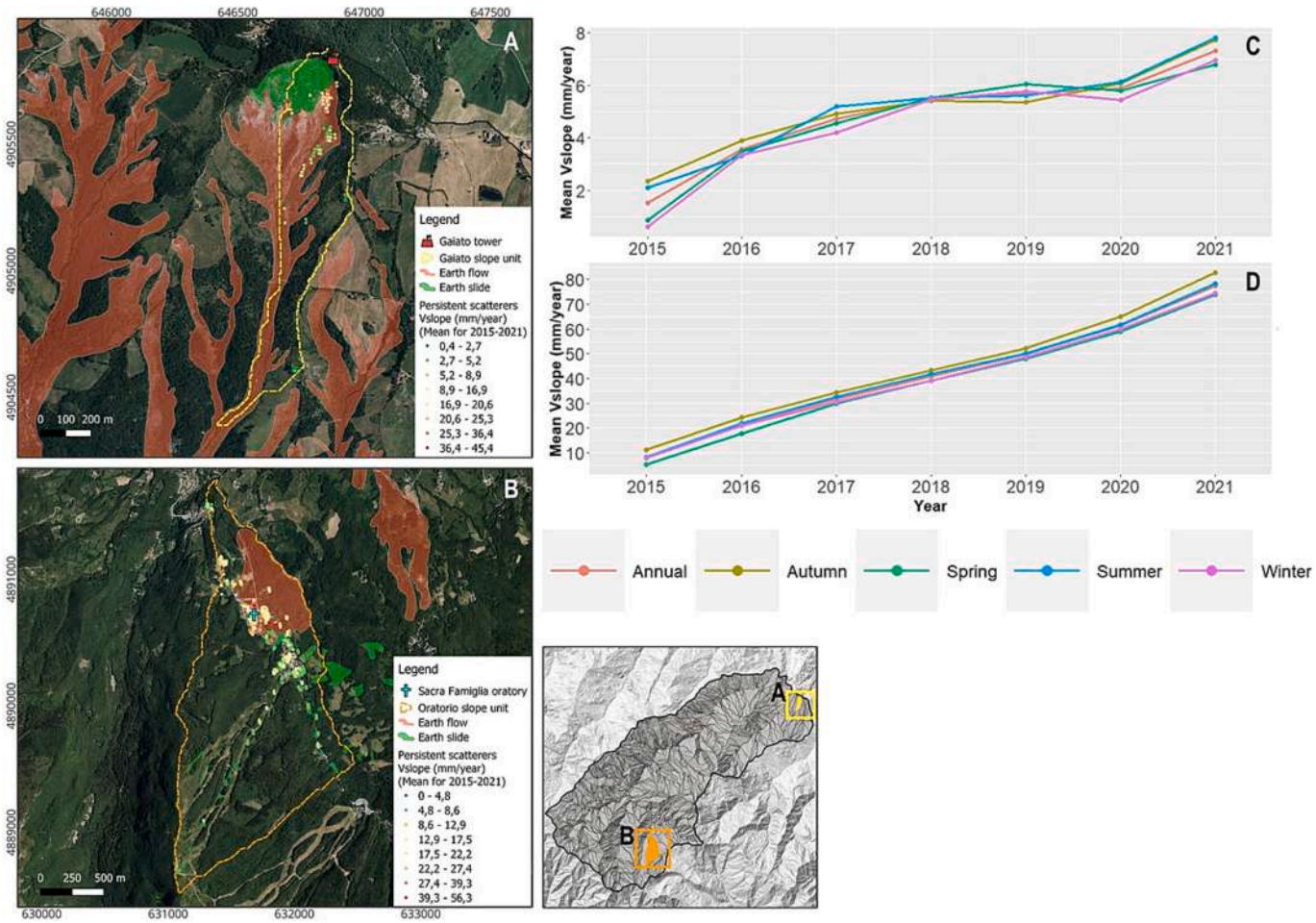

Fig. 10. Gaiato tower slope unit and distribution of PSI data (A); Oratory slope unit and distribution of PSI data (B); V_{slope} seasonal and annual means for the Gaiato slope unit (C) and the Oratory slope unit (D).

displacement rates take place during summer and autumn. For the Gaiato Tower SU, we outline two hypotheses to explain the observed seasonal pattern of displacement: a) it could be related to the time that rainfall water takes to infiltrate and reach the rupture surfaces associated with the underlying clay formations; and b) the higher observed displacements during the summer could be related to the drying of the clay formations, resulting in a vertical displacement of the landslide body. Those hypotheses could be further tested in future studies by detailed geotechnical and geomorphological surveys in the area. In the oratory SU, we associate the higher and constant displacement rates to the higher annual rainfall and a potential contribution of snowmelt.

Our approach shows the potential of the integration of quantitative susceptibility modeling with PSI data for the identification of potentially landslide-affected built environments in a cost- and time-effective method, that can be entirely reproduced with open-source data and software in different geomorphological and climatic contexts. The SU-level susceptibility map allows the acquisition of a catchment-wide notion of the potential landslide effects on buildings, while the use of data from MT-DInSAR provides a more detailed assessment of the sites that are potentially affected by past and current phenomena. Our approach applicability is not restricted to cultural heritage sites but could be reproduced for any other type of built environment. The two case studies show that the method is applicable in areas with different geomorphological and land cover characteristics.

On the other hand, two main drawbacks can be highlighted. The first one is related to the inevitable simplification of the landslide style of activity involved in susceptibility modeling (Guzzetti et al., 1999; Corominas et al., 2014), such as in the case of the Gaiato landslide. However, this can be considered a minor limitation for this research since the simplification is supported by field evidence and the susceptibility map's purpose was to provide a wider view of landslide dynamics in the area. In other geomorphological and climatic contexts where complex landslides are less frequent this limitation should not be a serious issue.

The second limitation is related to the interferometric data. The EGMS data has a limitation for the monitoring of ongoing displacements since the datasets are updated every 12 months due to the continental scale of the EGMS project (Crosetto and Solari, 2023). Nevertheless, our approach is useful for identifying cultural heritage and other built structures whose slopes have higher displacement rates in the time series provided by the EGMS. For those slopes, the second limitation can be overcome by processing recent SAR data aiming to monitor ongoing processes as suggested by Crosetto and Solari (2023). Such an approach results also in a less computationally intensive process due to the smaller size of the SAR datasets that need to be analyzed (i.e., the areas previously identified in the EGMS data with higher displacements). Additionally, the analysis of recent SAR datasets could be done using higher-resolution SAR products aiming to better depict the spatio-temporal distribution of displacements.

6. Conclusions

In this paper, we integrated landslide susceptibility assessment and interferometric data to identify cultural heritage sites potentially

affected by landslides. We tested this approach in a catchment of the Modena Apennines (Italy) that is affected mainly by earth slides and earth flows. Our results show that most of the cultural heritage sites are situated in areas with low to moderately low susceptibility to the analyzed landslide types. However, floods and other geomorphic processes whose analysis was outside of the scope of this paper can potentially affect those sites' integrity and could be analyzed in a future multihazard study. Eighteen sites are located on terrains with the highest susceptibility level and five of them displayed high displacement rates in the analyzed time frame (2015–2021).

Therefore, the main advantages of our proposal are its reproducibility and flexibility, since only open data and open software were used to achieve the results. This characteristic allows the identification of the potential consequences of natural hazards to built environments efficiently and cost-effectively. The proposed workflow can be applied in diverse geomorphological and climatic contexts, considering other landslide types, other geomorphic processes, and also structures other than cultural heritage sites. In summary, this study provides insights into landslide susceptibility and state of activity, demonstrating the potential for practical application for the evaluation of the potential effects of landslides on built environments.

CRediT authorship contribution statement

José Eduardo Bonini: Writing – review & editing, Writing – original draft, Visualization, Validation, Software, Resources, Project administration, Methodology, Investigation, Funding acquisition, Formal analysis, Data curation, Conceptualization. **Carlotta Parenti:** Writing – review & editing, Writing – original draft, Resources, Methodology, Investigation, Formal analysis, Conceptualization. **Francesca Grassi:** Writing – review & editing, Writing – original draft, Validation, Software, Resources, Methodology, Investigation, Formal analysis, Data curation, Conceptualization. **Francesco Mancini:** Writing – review & editing, Supervision, Resources, Conceptualization. **Bianca Carvalho Vieira:** Writing – review & editing, Supervision, Project administration, Funding acquisition, Conceptualization. **Mauro Soldati:** Writing – review & editing, Supervision, Resources, Project administration, Funding acquisition, Conceptualization.

Declaration of competing interest

The authors declare the following financial interests/personal relationships which may be considered as potential competing interests: Jose Eduardo Bonini reports financial support was provided by State of Sao Paulo Research Foundation. Mauro Soldati reports financial support was provided by University of Modena and Reggio Emilia. If there are other authors, they declare that they have no known competing financial interests or personal relationships that could have appeared to influence the work reported in this paper.

Acknowledgments

This research originates from a collaboration between the Graduate Program in Physical Geography of the University of São Paulo (Brazil) and the Department of Chemical and Geological Sciences of the University of Modena and Reggio Emilia (Unimore) (Italy) in the frame of the Research Internship Abroad and the Ph.D research project both funded by the FAPESP (grant #2022/13591-6 and grant #2021/04621-6, São Paulo Research Foundation). The research is also part of the project “Deciphering the response of the slope-fluvial system to environmental changes: Toward effective forecasting and Prevention of hydrogeological RIsks in the Modena Apennines (PRIMA)” funded by the University of Modena and Reggio Emilia, and the Fondazione di Modena in the frame of the “Fondo di Ateneo per la Ricerca 2023 - Progetti di Ricerca Interdisciplinare – Linea FOMO” (Scientific responsible: M. Soldati). The authors also thank the two anonymous reviewers for their suggestions.

Data availability

No data was used for the research described in the article.

References

Abbate, E., Bortolotti, V., Passerini, P., Sagri, M., 1970. Introduction to the geology of the Northern Apennines. Sediment. Geol. 4, 207–249. https://doi.org/10.1016/0037-0738(70)90017-5.

Agapiou, A., Lysandrou, V., Alexakis, D.D., Themistocleous, K., Cuca, B., Argyriou, A., Sarris, A., Hadjimitsis, D.G., 2015. Cultural heritage management and monitoring using remote sensing data and GIS: the case study of Paphos area, Cyprus. Comput. Environ. Urban. Syst. 54, 230–239. https://doi.org/10.1016/j.compenvurbsys.2015.09.003.

Amato, V., Aucelli, P.P.C., Corrado, G., Di Paola, G., Matano, F., Pappone, G., Schiattarella, M., 2020. Comparing geological and Persistent Scatterer Interferometry data of the Sele River coastal plain, southern Italy: implications for recent subsidence trends. Geomorphology 351, 106953. https://doi.org/10.1016/j.geomorph.2019.106953.

APAT, Agenzia per la Protezione dell''Ambiente e per i Servizi Tecnici, 2004. Rapporto sulle frane in Italia: il Progetto IFFI – metodologia, risultati e rapporti regionali. In: APAT Report, vol. 78 (681 pp.).

Ayalew, L., Yamagishi, H., 2005. The application of GIS-based logistic regression for landslide susceptibility mapping in the Kakuda-Yahiko Mountains, Central Japan. Geomorphology 65, 15–31. https://doi.org/10.1016/j.geomorph.2004.06.010.

Barella, C.F., Sobreira, F.G., Zêzere, J.L., 2019. A comparative analysis of statistical landslide susceptibility mapping in the southeast region of Minas Gerais state, Brazil. Bull. Eng. Geol. Environ. 78, 3205–3221. https://doi.org/10.1007/s10064-018-1341-3.

Bertolini, G., Pellegrini, M., 2001. The landslides of the Emilia Apennines (northern Italy) with reference to those which resumed activity in the 1994–1999 period and required Civil Protection interventions. Quaderni di Geologia Applicata 2, 27–74.

Bertolini, G., Canuti, P., Casagli, N., De Nardo, M.T., Egidi, D., Mainetti, M., Pignone, R., Pizziolo, M., 2002. Carta della Pericolosità Relativa da Frana della Regione Emilia-Romagna. SystemCart, Rome, Italy.

Bertolini, G., Guida, M., Pizziolo, M., 2005. Landslides in Emilia-Romagna region (Italy): strategies for hazard assessment and risk management. Landslides 2, 302–312. https://doi.org/10.1007/s10346-005-0020-1.

Bertolini, G., Corsini, A., Tellini, C., 2017. Fingerprints of large-scale landslides in the landscape of the Emilia Apennines. In: Soldati, M., Marchetti, M. (Eds.), Landscapes and Landforms of Italy, World Geomorphological Landscapes. Springer, Cham, Switzerland, pp. 215–224. https://doi.org/10.1007/978-3-319-26194-2_18.

Bianchini, S., Herrera, G., Mateos, R., Notti, D., Garcia, I., Mora, O., Moretti, S., 2013. Landslide activity maps generation by means of Persistent Scatterer Interferometry. Remote Sens. 5, 6198–6222. https://doi.org/10.3390/rs5126198.

Bonini, J.E., Bateira, C.V. de M., Dias, V.C., Martins, T.D., Vieira, B.C., 2020. Suscetibilidade a escorregamentos rasos a partir de parâmetros morfométricos e dos modelos SHALSTAB e do Valor Informativo. Confins. https://doi.org/10.4000/confins.30323.

Bonini, J.E., Vieira, B.C., Corrêa, A.C. de B., Soldati, M., 2023. Landslides and cultural heritage – a review. Heritage 6 (10), 6648–6668. https://doi.org/10.3390/heritage6100348.

Borgatti, L., Soldati, M., 2005. Fenomeni franosi. In: Panizza, M. (Ed.), Manuale di Geomorfologia Applicata. Franco Angeli, Milan, pp. 88–123.

Borgatti, L., Soldati, M., 2010. Landslides and climatic change. In: Alcántara-Ayala, I., Goudie, A. (Eds.), Geomorphological Hazards and Disaster Prevention. Cambridge University Press, Cambridge, MA, USA, pp. 87–95.

Brabb, E.E., 1984. Innovative approaches to landslide hazard mapping. In: 4th International Symposium on Landslides, 16 a 21 de September. Toronto, Canada, pp. 307–324.

Bradley, A.P., 1997. The use of the area under the ROC curve in the evaluation of machine-learning algorithms. Pattern Recogn. 30, 1145–1159. https://doi.org/10.1515/bchm.1997.378.7.697.

Breiman, L.E.O., 2001. Random forests. In: Machine-learning, vol. 45, pp. 5–32. https://doi.org/10.1023/A:1010933404324.

Brock, J., Schratz, P., Petschko, H., Muenchow, J., Micu, M., Brenning, A., 2020. The performance of landslide susceptibility models critically depends on the quality of digital elevation models. Geomat. Nat. Hazards Risk 11, 1075–1092. https://doi.org/10.1080/19475705.2020.1776403.

Broeckx, J., Vanmaercke, M., Duchateau, R., Poesen, J., 2018. A data-based landslide susceptibility map of Africa. Earth Sci. Rev. 185, 102–121. https://doi.org/10.1016/J.EARSCIREV.2018.05.002.

Bui, D.T., Tsangaratos, P., Nguyen, V.T., Liem, N.V., Trinh, P.T., 2020. Comparing the prediction performance of a Deep Learning Neural Network model with conventional machine-learning models in landslide susceptibility assessment. Catena 188, 104426. https://doi.org/10.1016/j.catena.2019.104426.

Cancelli, A., Pellegrini, M., Tosattl, G., 1987. Alcuni esempi di deformazioni gravitative profonde di versante nell'Appennino Settentrionale. In: Memorie della Società Geologica Italiana, vol. 39, pp. 447–466.

Carlà, T., Tofani, V., Lombardi, L., Raspini, F., Bianchini, S., Bertolo, D., Thuegaz, P., Casagli, N., 2019. Combination of GNSS, satellite InSAR, and GBInSAR remote sensing monitoring to improve the understanding of a large landslide in high alpine

environment. Geomorphology 335, 62–75. https://doi.org/10.1016/j.geomorph.2019.03.014.
Carosi, R., Montomoli, C., Pertusati, P.C., 2004. Late tectonic evolution of the Northern Apennines: the role of contractional tectonics in the exhumation of the Tuscan units. Geodin. Acta 17 (4), 253–273. https://doi.org/10.3166/ga.17.253-273.
Carrara, A., 1983. Multivariate models for landslide hazard evaluation. Math. Geol. 15, 403–426. https://doi.org/10.1007/BF01031290.
Carrara, A., Cardinali, M., Detti, R., Guzzetti, F., Pasqui, V., Reichenbach, P., 1991. GIS techniques and statistical models in evaluating landslide hazard. Earth Surf. Process. Landf. 16, 427–445. https://doi.org/10.1002/esp.3290160505.
Cascini, L., Fornaro, G., Peduto, D., 2010. Advanced low- and full-resolution DInSAR map generation for slow-moving landslide analysis at different scales. Eng. Geol. 112 (1–4), 9–42. https://doi.org/10.1016/j.enggeo.2010.01.003.
Castaldini, D., Ghinoi, A., Maccaferri, A., 2012. Considerations on geomorphological maps for territorial planning in the Modena Apennines (Northern Italy). Nat. Hazards Earth Syst. Sci. 12, 421–430. https://doi.org/10.5194/nhess-12-421-2012.
Chalkias, C., Polykretis, C., Karymbalis, E., Soldati, M., Ghinoi, A., Ferentinou, M., 2020. Exploring spatial non-stationarity in the relationships between landslide susceptibility and conditioning factors: a local modeling approach using geographically weighted regression. Bull. Eng. Geol. Environ. 79, 2799–2814. https://doi.org/10.1007/s10064-020-01733-x.
Chen, T., Niu, R., Jia, X., 2016. A comparison of information value and logistic regression models in landslide susceptibility mapping by using GIS. Environ. Earth Sci. 75, 867. https://doi.org/10.1007/s12665-016-5317-y.
Chen, W., Pourghasemi, H.R., Kornejady, A., Zhang, N., 2017. Landslide spatial modeling: Introducing new ensembles of ANN, MaxEnt, and SVM machine-learning techniques. Geoderma 305, 314–327. https://doi.org/10.1016/j.geoderma.2017.06.020.
Ciampalini, A., Raspini, F., Frodella, W., 2016a. Back monitoring of the San Leo (northern Italy) rock cliff by means of SqueeSAR technique. Rend. Online Soc. Geol. Ital. 41, 227–230. https://doi.org/10.3301/ROL.2016.135.
Ciampalini, A., Raspini, F., Frodella, W., Bardi, F., Bianchini, S., Moretti, S., 2016b. The effectiveness of high-resolution LiDAR data combined with PSInSAR data in landslide study. Landslides 13, 399–410. https://doi.org/10.1007/s10346-015-0663-5.
Cigna, F., Jordan, H., Bateson, L., McCormack, H., Roberts, C., 2015. Natural and anthropogenic geohazards in greater London observed from geological and ERS-1/2 and ENVISAT persistent scatterers ground motion data: results from the EC FP7-SPACE PanGeo project. Pure Appl. Geophys. 172, 2965–2995. https://doi.org/10.1007/s00024-014-0927-3.
Cignetti, M., Godone, D., Notti, D., Giordan, D., Bertolo, D., Calò, F., Reale, D., Verde, S., Fornaro, G., 2023. State of activity classification of deep-seated gravitational slope deformation at regional scale based on Sentinel-1 data. Landslides 20, 2529–2544. https://doi.org/10.1007/s10346-023-02114-7.
Colesanti, C., Wasowski, J., 2006. Investigating landslides with space-borne Synthetic Aperture Radar (SAR) interferometry. Eng. Geol. 88, 173–199. https://doi.org/10.1016/j.enggeo.2006.09.013.
Corominas, J., van Westen, C., Frattini, P., Cascini, L., Malet, J.-P., Fotopoulou, S., Catani, F., Van Den Eeckhaut, M., Mavrouli, O., Agliardi, F., Pitilakis, K., Winter, M. G., Pastor, M., Ferlisi, S., Tofani, V., Hervás, J., Smith, J.T., 2014. Recommendations for the quantitative analysis of landslide risk. Bull. Eng. Geol. Environ. 73, 209–263. https://doi.org/10.1007/s10064-013-0538-8.
Crosetto, M., Solari, L., 2023. European ground motion service. In: Satellite Interferometry Data Interpretation and Exploitation. Elsevier, pp. 63–87. https://doi.org/10.1016/B978-0-443-13397-8.00003-0.
Crosetto, M., Solari, L., Mróz, M., Balasis-Levinsen, J., Casagli, N., Frei, M., Oyen, A., Moldestad, D.A., Bateson, L., Guerrieri, L., Comerci, V., Andersen, H.S., 2020. The evolution of wide-area DInSAR: from regional and national services to the European Ground Motion Service. Remote Sens. 12, 2043. https://doi.org/10.3390/rs12122043.
Crozier, M., 1986. Landslides: Causes, Consequences and Environment. Croom Helm Australia Pty. Ltd., London.
Crozier, M.J., 2010. Landslide geomorphology: an argument for recognition, with examples from New Zealand. Geomorphology 120, 3–15. https://doi.org/10.1016/j.geomorph.2009.09.010.
Cruden, D.M., Varnes, D.J., 1996. Landslide types and processes. In: Turner, A.K., Schuster, R.L. (Eds.), Landslides and Engineering Practice, Transportation Research Board, US National Academy of Sciences, Special Report, 247: 36–75, Washington D. C, pp. 20–47.
Dammag, B.Q.D., Jian, D., Dammag, A.Q., 2024. Cultural heritage sites risk assessment and management using a hybridized technique based on GIS and SWOT-AHP in the Ancient City of Ibb, Yemen. Int. J. Archit. Herit. 1–36. https://doi.org/10.1080/15583058.2024.2364717.
El-Fengour, A., Bateira, C., El Motaki, H., García, H., 2021. Landslide susceptibility assessment based on information value model in Amzaz Watershed in Northern Morocco. Physis Terrae 2, 3–19. https://doi.org/10.21814/physisterrae.2965.
Fawcett, T., 2006. An introduction to ROC analysis. Pattern Recogn. Lett. 27, 861–874. https://doi.org/10.1016/j.patrec.2005.10.010.
Ferretti, A., Prati, C., Rocca, F., 2001. Permanent scatterers in SAR interferometry. IEEE Trans. Geosci. Remote Sens. 39, 8–20. https://doi.org/10.1109/36.898661.
Gelmini, R., Pellegrini, M., 1969. Le frane del bacino del Panaro. In: Atti della Società dei Naturalisti e Matematici di Modena, 100, pp. 112–149.
Gigli, G., Frodella, W., Mugnai, F., Tapete, D., Cigna, F., Fanti, R., Intrieri, E., Lombardi, L., 2012. Instability mechanisms affecting cultural heritage sites in the Maltese Archipelago. Nat. Hazards Earth Syst. Sci. 12, 1883–1903. https://doi.org/10.5194/nhess-12-1883-2012.
Glade, Thomas, Crozier, M.J., 2005. The nature of landslide hazard and impact. In: Anderson, M.G., Crozier, M.J., Glade, T. (Eds.), Landslide Hazard and Risk. John Wiley and Sons, Chichester, pp. 43–74.
Goetz, J.N., Brenning, A., Petschko, H., Leopold, P., 2015. Evaluating machine-learning and statistical prediction techniques for landslide susceptibility modeling. Comput. Geosci. 81, 1–11. https://doi.org/10.1016/j.cageo.2015.04.007.
Guzzetti, F., Carrara, A., Cardinali, M., Reichenbach, P., 1999. Landslide hazard evaluation: a review of current techniques and their application in a multi-scale study, Central Italy. Geomorphology 31, 181–216. https://doi.org/10.1016/S0169-555X(99)00078-1.
Han, Hong, Guo, Xiaoling, Hua, Yu, 2016. Variable selection using mean decrease accuracy and mean decrease gini based on random forest. In: 2016 7th IEEE International Conference on Software Engineering and Service Science (ICSESS). Presented at the 2016 7th IEEE International Conference on Software Engineering and Service Science (ICSESS). IEEE, Beijing, China, pp. 219–224. https://doi.org/10.1109/ICSESS.2016.7883053.
Herrera, G., Gutiérrez, F., García-Davalillo, J.C., Guerrero, J., Notti, D., Galve, J.P., Fernández-Merodo, J.A., Cooksley, C., 2013. Multi-sensor advanced DInSAR monitoring of very slow landslides: the Tena Valley case study (Central Spanish Pyrenees). Remote Sens. Environ. 128, 31–43. https://doi.org/10.1016/j.rse.2012.09.020.
Hervás, J., Bobrowsky, P., 2009. Mapping: inventories, susceptibility, hazard and risk. In: Sassa, K., Canuti, P. (Eds.), Landslides – Disaster Risk Reduction. Springer, Berlin Heidelberg, Berlin, Heidelberg, pp. 321–349. https://doi.org/10.1007/978-3-540-69970-5_19.
Hong, H., Pradhan, B., Xu, C., Tien Bui, D., 2015. Spatial prediction of landslide hazard at the Yihuang area (China) using two-class kernel logistic regression, alternating decision tree and support vector machines. Catena 133, 266–281. https://doi.org/10.1016/j.catena.2015.05.019.
Hooper, A., Zebker, H., Segall, P., Kampes, B., 2004. A new method for measuring deformation on volcanoes and other natural terrains using InSAR persistent scatterers. Geophys. Res. Lett. 31, 2004GL021737. https://doi.org/10.1029/2004GL021737.
Iadanza, C., Trigila, A., Starace, P., Dragoni, A., Biondo, T., Roccisano, M., 2021. IdroGEO: a collaborative web mapping application based on rest api services and open data on landslides and floods in Italy. Int. J. Geo-Inf. 10, 89. https://doi.org/10.3390/ijgi10020089.
ICOMOS, International Council on Monuments and Sites, 2000. World Report 2000 on Monuments and Sites in Danger. ICOMOS, Berlin.
ICOMOS, International Council on Monuments and Sites, 2020. Heritage at Risk: World Report 2016–2019 on Monuments and Sites in Danger. Hendrik Bäßler verlag, Berlin.
Jade, S., Sarkar, S., 1993. Statistical models for slope instability classification. Eng. Geol. 36, 91–98. https://doi.org/10.1016/0013-7952(93)90021-4.
Jiao, Y., Zhao, D., Ding, Y., Liu, Y., Xu, Q., Qiu, Y., Liu, C., Liu, Z., Zha, Z., Li, R., 2019. Performance evaluation for four GIS-based models purposed to predict and map landslide susceptibility: a case study at a World Heritage site in Southwest China. Catena 183, 104221. https://doi.org/10.1016/j.catena.2019.104221.
Kim, J.W., Kim, H.G., 2021. Landslide susceptibility analysis by type of cultural heritage site using ensemble model: case study of the Chungcheong Region of South Korea. Sens. Mater. 33, 3819–3833. https://doi.org/10.18494/SAM.2021.3593.
Klimeš, J., 2013. Landslide temporal analysis and susceptibility assessment as bases for landslide mitigation, Machu Picchu, Peru. Environ. Earth Sci. 70, 913–925. https://doi.org/10.1007/s12665-012-2181-2.
Kohavi, R., 1995. A study of cross-validation and bootstrap for accuracy estimation and model selection. In: Proceedings of the 14th International Joint Conference on Artificial intelligence, vol. 2, pp. 1137–1143.
Köppen, W., 1931. Grundriß der Klimakunde, 2nd ed. Walter de Gruyter and Co., Berlin, Germany; Leipzig, Germany.
Kuhn, M., 2008. Building predictive models in R using the caret package. J. Stat. Softw. 28, 1–26. https://doi.org/10.18637/jss.v028.i05.
Lee, E.M., Jones, D.K.C., 2004. Landslide Risk Assessment. Thomas Telford Ltd. https://doi.org/10.1680/lra.31715
Liberatoscioli, E., Van Westen, C.J., Soldati, M., 2017. Assessment of landslide susceptibility for civil protection purposes by means of GIS and statistical analysis: lessons from the Province of Modena, Italy. Rev. Geomorfol. 19, 29–43. https://doi.org/10.21094/rg.2017.009.
Lombardo, L., Tanyas, H., Nicu, I.C., 2020. Spatial modeling of multi-hazard threat to cultural heritage sites. Eng. Geol. 277, 105776. https://doi.org/10.1016/j.enggeo.2020.105776.
Mancini, F., Ceppi, C., Ritrovato, G., 2010. GIS and statistical analysis for landslide susceptibility mapping in the Daunia area, Italy. Nat. Hazards Earth Syst. Sci. 10, 1851–1864. https://doi.org/10.5194/nhess-10-1851-2010.
Mancini, F., Grassi, F., Cenni, N., 2021. A workflow based on SNAP–StaMPS open-source tools and GNSS data for PSI-based ground deformation using dual-orbit sentinel-1 data: accuracy assessment with error propagation analysis. Remote Sens. 13, 753. https://doi.org/10.3390/rs13040753.
Mantovani, M., Devoto, S., Piacentini, D., Prampolini, M., Soldati, M., Pasuto, A., 2016. Advanced SAR interferometric analysis to support geomorphological interpretation of slow-moving coastal landslides (Malta, Mediterranean Sea). Remote Sens. 8, 443. https://doi.org/10.3390/rs8060443.
Massonnet, D., Feigl, K.L., 1998. Radar interferometry and its application to changes in the Earth's surface. Rev. Geophys. 36, 441–500. https://doi.org/10.1029/97RG03139.
Meng, S., Shi, Z., Li, G., Peng, M., Liu, L., Zheng, H., Zhou, C., 2024. A novel deep learning framework for landslide susceptibility assessment using improved deep

belief networks with the intelligent optimization algorithm. Comput. Geotech. 167, 106106. https://doi.org/10.1016/j.compgeo.2024.106106.
Micu, M., Micu, D., Soldati, M., 2022. Mass movements in changing mountainous environments. In: Shroder, J.F. (Ed.), Treatise on Geomorphology. Academic Press, Cambridge, MA, USA, pp. 371–388.
Mondini, A.C., Guzzetti, F., Chang, K.-T., Monserrat, O., Martha, T.R., Manconi, A., 2021. Landslide failures detection and mapping using Synthetic Aperture Radar: Past, present and future. Earth Sci. Rev. 216, 103574. https://doi.org/10.1016/j.earscirev.2021.103574.
Mulas, M., Ciccarese, G., Ronchetti, F., Truffelli, G., Corsini, A., 2018. Slope dynamics and streambed uplift during the Pergalla landslide reactivation in March 2016 and discussion of concurrent causes (Northern Apennines, Italy). Landslides 15, 1881–1887. https://doi.org/10.1007/s10346-018-1039-4.
Ng, A.H.-M., Liu, Z., Du, Z., Huang, H., Wang, H., Ge, L., 2023. A novel framework for combining polarimetric Sentinel-1 InSAR time series in subsidence monitoring - a case study of Sydney. Remote Sens. Environ. 295, 113694. https://doi.org/10.1016/j.rse.2023.113694.
Nicu, I.C., 2018. Application of analytic hierarchy process, frequency ratio, and statistical index to landslide susceptibility: an approach to endangered cultural heritage. Environ. Earth Sci. 77, 79. https://doi.org/10.1007/s12665-018-7261-5.
Nicu, I.C., Asandulesei, A., 2018. GIS-based evaluation of diagnostic areas in landslide susceptibility analysis of Bahluiet River Basin (Moldavian Plateau, NE Romania). Are Neolithic sites in danger? Geomorphology 314, 27–41. https://doi.org/10.1016/j.geomorph.2018.04.010.
Notti, D., Herrera, G., Bianchini, S., Meisina, C., García-Davalillo, J.C., Zucca, F., 2014. A methodology for improving landslide PSI data analysis. Int. J. Remote Sens. 35, 2186–2214. https://doi.org/10.1080/01431161.2014.889864.
Parenti, C., Rossi, P., Mancini, F., Scorpio, V., Grassi, F., Ciccarese, G., Lugli, F., Soldati, M., 2023. Multitemporal analysis of slow-moving landslides and channel dynamics through integrated remote sensing and in situ techniques. Remote Sens. 15, 3563. https://doi.org/10.3390/rs15143563.
Pastonchi, L., Barra, A., Monserrat, O., Luzi, G., Solari, L., Tofani, V., 2018. Satellite data to improve the knowledge of geohazards in world heritage sites. Remote Sens. 10, 992. https://doi.org/10.3390/rs10070992.
Pasuto, A., Soldati, M., 1996. Landslide hazard. In: Panizza, M. (Ed.), Environmental Geomorphology. Elsevier, Amsterdam, pp. 64–88.
Pawley, S., 2023. Rsagacmd: Linking R With the Open-Source "SAGA-GIS" Software. R Package Version.
Petschko, H., Brenning, A., Bell, R., Goetz, J., Glade, T., 2014. Assessing the quality of landslide susceptibility maps - case study Lower Austria. Nat. Hazards Earth Syst. Sci. 14, 95–118. https://doi.org/10.5194/nhess-14-95-2014.
Piacentini, D., Troiani, F., Soldati, M., Notarnicola, C., Savelli, D., Schneiderbauer, S., Strada, C., 2012. Statistical analysis for assessing shallow-landslide susceptibility in South Tyrol (south-eastern Alps, Italy). Geomorphology 151–152, 196–206. https://doi.org/10.1016/j.geomorph.2012.02.003.
Piacentini, D., Devoto, S., Mantovani, M., Pasuto, A., Prampolini, M., Soldati, M., 2015. Landslide susceptibility modeling assisted by Persistent Scatterers Interferometry (PSI): an example from the northwestern coast of Malta. Nat. Hazards 78, 681–697. https://doi.org/10.1007/s11069-015-1740-8.
Piacentini, D., Troiani, F., Daniele, G., Pizziolo, M., 2018. Historical geospatial database for landslide analysis: the Catalogue of Landslide OCcurrences in the Emilia-Romagna Region (CLOCkER). Landslides 15, 811–822. https://doi.org/10.1007/s10346-018-0962-8.
Pourghasemi, H.R., Rahmati, O., 2018. Prediction of the landslide susceptibility: which algorithm, which precision? Catena 162, 177–192. https://doi.org/10.1016/j.catena.2017.11.022.
Pourghasemi, H.R., Jirandeh, A.G., Pradhan, B., Xu, C., Gokceoglu, C., 2013. Landslide susceptibility mapping using support vector machine and GIS at the Golestan Province, Iran. J. Earth Syst. Sci. 122, 349–369. https://doi.org/10.1007/s12040-013-0282-2.
Qiao, X., Chu, T., Tissot, P., Holland, S., 2023. Sentinel-1 InSAR-derived land subsidence assessment along the Texas Gulf Coast. Int. J. Appl. Earth Obs. Geoinf. 125, 103544. https://doi.org/10.1016/j.jag.2023.103544.
R Core Team, 2019. R: a language and environment for statistical computing, R Foundation for Statistical Computing, Vienna. https://www.R-project.org.
Raspini, F., Loupasakis, C., Rozos, D., Adam, N., Moretti, S., 2014. Ground subsidence phenomena in the Delta municipality region (Northern Greece): geotechnical modeling and validation with Persistent Scatterer Interferometry. Int. J. Appl. Earth Obs. Geoinf. 28, 78–89. https://doi.org/10.1016/j.jag.2013.11.010.
Reale, D., Noviello, C., Verde, S., Cascini, L., Terracciano, G., Arena, L., 2019. A multi-disciplinary approach for the damage analysis of cultural heritage: the case study of the St. Gerlando Cathedral in Agrigento. Remote Sens. Environ. 235, 111464. https://doi.org/10.1016/j.rse.2019.111464.
Reichenbach, P., Rossi, M., Malamud, B.D., Mihir, M., Guzzetti, F., 2018. A review of statistically-based landslide susceptibility models. Earth Sci. Rev. 180, 60–91. https://doi.org/10.1016/j.earscirev.2018.03.001.
Ronchetti, F., Borgatti, L., Cervi, F., Lucente, C.C., Veneziano, M., Corsini, A., 2007. The Valoria landslide reactivation in 2005–2006 (Northern Apennines, Italy). Landslides 4, 189–195. https://doi.org/10.1007/s10346-006-0073-9.
Rosi, A., Tofani, V., Agostini, A., Tanteri, L., Tacconi Stefanelli, C., Catani, F., Casagli, N., 2016. Subsidence mapping at regional scale using persistent scatters interferometry (PSI): The case of Tuscany region (Italy). Int. J. Appl. Earth Obs. Geoinf. 52, 328–337. https://doi.org/10.1016/j.jag.2016.07.003.
Saha, A., Pal, S.C., Santosh, M., Janizadeh, S., Chowdhuri, I., Norouzi, A., Roy, P., Chakrabortty, R., 2021. Modelling multi-hazard threats to cultural heritage sites and environmental sustainability: the present and future scenarios. J. Clean. Prod. 320. https://doi.org/10.1016/j.jclepro.2021.128713.
Saha, S., Majumdar, P., Bera, B., 2023. Deep learning and benchmark machine-learning based landslide susceptibility investigation, Garhwal Himalaya (India). Quat. Sci. Adv. 10, 100075. https://doi.org/10.1016/j.qsa.2023.100075.
Sameen, M.I., Pradhan, B., 2019. Landslide detection using residual networks and the fusion of spectral and topographic information. IEEE Access 7, 114363–114373. https://doi.org/10.1109/ACCESS.2019.2935761.
Sdao, F., Lioi, D.S., Pascale, S., Caniani, D., Mancini, I.M., 2013. Landslide susceptibility assessment by using a neuro-fuzzy model: a case study in the Rupestrian heritage rich area of Matera. Nat. Hazards Earth Syst. Sci. 13, 395–407. https://doi.org/10.5194/nhess-13-395-2013.
Soeters, R., van Westen, C.J., 1996. Slope instability recognition, analysis, and zonation, 129–177. In: Turner, A.K., Schuster, R.L. (Eds.), Landslides, Investigation and Mitigation, Transportation Research Board Special Report, vol. 247. National Academy Press.
Soldati, M., 1997. Aspetti geomorfologici. In: Dondi, C., Dotti, R., Rompianesi, G. (Eds.), 2° Relazione sullo stato dell'ambiente nella provincia di Modena. Provincia di Modena, pp. 23–28.
Steger, S., Brenning, A., Bell, R., Petschko, H., Glade, T., 2016. Exploring discrepancies between quantitative validation results and the geomorphic plausibility of statistical landslide susceptibility maps. Geomorphology 262, 8–23. https://doi.org/10.1016/j.geomorph.2016.03.015.
Steger, S., Brenning, A., Bell, R., Glade, T., 2017. The influence of systematically incomplete shallow landslide inventories on statistical susceptibility models and suggestions for improvements. Landslides 14, 1767–1781. https://doi.org/10.1007/s10346-017-0820-0.
Tarragüel, A.A., Krol, B., van Westen, C., 2012. Analyzing the possible impact of landslides and avalanches on cultural heritage in Upper Svaneti, Georgia. J. Cult. Herit. 13 (4), 453–461. https://doi.org/10.1016/j.culher.2012.01.012.
Teatini, P., Tosi, L., Strozzi, T., Carbognin, L., Cecconi, G., Rosselli, R., Libardo, S., 2012. Resolving land subsidence within the Venice Lagoon by persistent scatterer SAR interferometry. Phys. Chem. Earth, Parts A/B/C 40–41, 72–79. https://doi.org/10.1016/j.pce.2010.01.002.
Terranova, C., Ventura, G., Vilardo, G., 2015. Multiple causes of ground deformation in the Napoli metropolitan area (Italy) from integrated Persistent Scatterers DinSAR, geological, hydrological, and urban infrastructure data. Earth Sci. Rev. 146, 105–119. https://doi.org/10.1016/j.earscirev.2015.04.001.
Themistocleous, K., Cuca, B., Agapiou, A., Lysandrou, V., Tzouvaras, M., Hadjimitsis, D. G., Kyriakides, P., Kouhartsiouk, D., Margottini, C., Spizzichino, D., Cigna, F., Crosta, G., Frattini, P., Merodo, J.A.F., 2016. The protection of cultural heritage sites from geo-hazards: the PROTHEGO project. In: Lecture Notes in Computer Science (Including subseries Lecture Notes in Artificial Intelligence and Lecture Notes in Bioinformatics) 10059 LNCS, pp. 91–98. https://doi.org/10.1007/978-3-319-48974-2_11.
Themistocleous, K., Danezis, C., Mendonidis, E., Lymperopoulou, E., 2017. Monitoring ground deformation of cultural heritage sites using UAVs and geodetic techniques: the case study of Choirokoitia, JPI PROTHEGO project. In: Michel, U., Schulz, K., Nikolakopoulos, K., Civco, D. (Eds.), Earth Resources and Environmental Remote Sensing/GIS Applications VIII, Proceedings of SPIE. https://doi.org/10.1117/12.2279478.
Themistocleous, K., Danezis, C., Gikas, V., 2021. Monitoring ground deformation of cultural heritage sites using SAR and geodetic techniques: the case study of Choirokoitia, Cyprus. Appl. Geomat. 13, 37–49. https://doi.org/10.1007/s12518-020-00329-0.
Tosatti, G., 1982. Una frana in arenarie fratturate e in argille con inclusi litoidi: la frana di Gaiato nell'Apennino Modenese. In: Atti della Società dei Naturalisti e Matematici di Modena, vol. 113, pp. 67–89.
Trigila, A., Iadanza, C., Spizzichino, D., 2010. Quality assessment of the Italian Landslide Inventory using GIS processing. Landslides 7, 455–470. https://doi.org/10.1007/s10346-010-0213-0.
Turner, A.K., Schuster, R.L., 1996. Landslides: Investigation and Mitigation. Special Report 247. Transportation Research Board, National Research Council, Washington D. C.
UNESCO, 1972. Convention Concerning the Protection of the World Cultural and Natural Heritage. UNESCO World Heritage Centre, Paris, France.
UNESCO, ICCROM, ICOMOS, IUCN, 2010. Managing Disaster Risks for World Heritage. UNESCO, Paris, France.
Van Dao, D., Jaafari, A., Bayat, M., Mafi-Gholami, D., Qi, C., Moayedi, H., Phong, T.V., Ly, H.B., Le, T.T., Trinh, P.T., Luu, C., Quoc, N.K., Thanh, B.N., Pham, B.T., 2020. A spatially explicit deep learning neural network model for the prediction of landslide susceptibility. Catena 188, 104451. https://doi.org/10.1016/j.catena.2019.104451.
van Westen, C.J., Castellanos, E., Kuriakose, S.L., 2008. Spatial data for landslide susceptibility, hazard, and vulnerability assessment: an overview. Eng. Geol. 102, 112–131. https://doi.org/10.1016/j.enggeo.2008.03.010.
Wang, T., DeGrandpre, K., Lu, Z., Freymueller, J.T., 2018. Complex surface deformation of Akutan volcano, Alaska revealed from InSAR time series. Int. J. Appl. Earth Obs. Geoinf. 64, 171–180. https://doi.org/10.1016/j.jag.2017.09.001.
Wasowski, J., Bovenga, F., 2014. Investigating landslides and unstable slopes with satellite Multi Temporal Interferometry: current issues and future perspectives. Eng. Geol. 174, 103–138. https://doi.org/10.1016/j.enggeo.2014.03.003.
Woodard, J.B., Mirus, B.B., Wood, N.J., Allstadt, K.E., Leshchinsky, B.A., Crawford, M. M., 2024. Slope Unit Maker (SUMak): an efficient and parameter-free algorithm for delineating slope units to improve landslide modeling. Nat. Hazards Earth Syst. Sci. 24, 1–12. https://doi.org/10.5194/nhess-24-1-2024.

Wu, Z., Ma, P., Zheng, Y., Gu, F., Liu, L., Lin, H., 2023. Automatic detection and classification of land subsidence in deltaic metropolitan areas using distributed scatterer InSAR and Oriented R-CNN. Remote Sens. Environ. 290, 113545. https://doi.org/10.1016/j.rse.2023.113545.

Xu, C., Xu, X., Dai, F., Saraf, A.K., 2012. Comparison of different models for susceptibility mapping of earthquake triggered landslides related with the 2008 Wenchuan earthquake in China. Comput. Geosci. 46, 317–329. https://doi.org/10.1016/j.cageo.2012.01.002.

Yang, J., You, Y., Ye, X., Lin, J., 2023. Cultural heritage sites risk assessment based on RS and GIS – takes the Fortified Manors of Yongtai as an example. Int. J. Disaster Risk Reduct. 88, 103593. https://doi.org/10.1016/j.ijdrr.2023.103593.

Yang, Q., Wang, X., Yin, J., Du, A., Zhang, A., Wang, L., Guo, H., Li, D., 2024. A novel CGBoost deep learning algorithm for coseismic landslide susceptibility prediction. Geosci. Front. 15, 101770. https://doi.org/10.1016/j.gsf.2023.101770.

Yin, K.L., Yan, T.Z., 1988. Statistical prediction models for slope instability of metamorphosed rocks. In: Bonnard, L. (Ed.), Fifth International Symposium on Landslides. Balkema, Rotterdam, Lausanne, pp. 1269–1272.

Yu, L., Wang, Y., Pradhan, B., 2024. Enhancing landslide susceptibility mapping incorporating landslide typology via stacking ensemble machine-learning in Three Gorges Reservoir, China. Geosci. Front., 101802 https://doi.org/10.1016/j.gsf.2024.101802.

Zêzere, J.L., Pereira, S., Melo, R., Oliveira, S.C., Garcia, R.A.C., 2017. Mapping landslide susceptibility using data-driven methods. Sci. Total Environ. 589, 250–267. https://doi.org/10.1016/j.scitotenv.2017.02.188.

Zhou, X., Wen, H., Zhang, Y., Xu, J., Zhang, W., 2021. Landslide susceptibility mapping using hybrid random forest with GeoDetector and RFE for factor optimization. Geosci. Front. 12, 101211. https://doi.org/10.1016/j.gsf.2021.101211.

Zhou, L., Wei, B., Chen, G., Liu, S., Li, X., Luo, Z., Qin, D., Zhang, D., 2024. InSAR time series analysis of natural and anthropogenic coastal plain subsidence: a case of Hangjiahu plain. Geod. Geodyn., S167498472400003X https://doi.org/10.1016/j.geog.2023.12.005.